치의과학 박사학위논문

# Identification of human vitronectin-derived dimeric peptide and its effects on modulation of osteoclast differentiation

# 인간 비트로넥틴 유래 이량체 펩티드 발굴 및 파골세포 분화 조절에 미치는 효과

2020년 8월


서울대학교 대학원

치의과학과 종양및발달생물학 전공

정 성 윤

# Identification of human vitronectin-derived dimeric peptide and its effects on modulation of osteoclast differentiation

지도교수 민 병 무

이 논문을 치의과학 박사학위논문으로 제출함

2020년 5월

서울대학교 대학원

치의과학과 종양및발달생물학 전공

정 성 윤

정성윤의 박사학위논문을 인준함

2020년 7월

위 원 장 _____ (인)

부위원장 _____ (인)

위 원 _____ (인)

위 원 _____ (인)

위 원 _____ (인)

# ABSTRACT

## Identification of human vitronectin-derived dimeric peptide and its effects on modulation of osteoclast differentiation

Sung-Youn Jung

Department of Cancer and Developmental Biology

Graduate School

Seoul National University

(Directed by Prof. Byung-Moo Min, D.D.S., M.S., Ph.D.)

Short bioactive peptides derived from extracellular matrix proteins are useful and attractive therapeutic agents for regenerative medicine and tissue engineering. Due to the various advantages of peptides, including their low cost, immunogenicity, and structural or functional flexibility, many studies have attempted to use them as regenerative medicine agents and to treat diseases. Attachment of cells to specific substrates is crucial for the modulation of specific cell responses in biomaterial design and development. Therefore, the identification of bioactive peptides that promote cell attachment is a critical strategy for bioactive peptide screening. Here, an IDAAFTRINCQG motif (VnP-

8, residues 206-217), which promotes cell attachment, was identified in the hemopexin-like domain 1 of human vitronectin. Through spontaneous air oxidation reaction, the 12-mer monomeric peptide, VnP-8, was transformed into an 11-mer dimeric peptide (VnP-8-DN1 dimer) by removing the isoleucine residue at the N-terminus of VnP-8 and then forming a disulfide bond between cysteine residues. The VnP-8-DN1 dimeric peptide strongly enhanced cell attachment activity, and dimeric peptide-mediated cell attachment was significantly inhibited by heparin, which antagonizes heparan sulfate proteoglycan, and is slightly blocked by ethylenediaminetetraacetic acid, an integrin-ligand binding inhibitor. Furthermore, the VnP-8-DN1 dimer inhibited the macrophage-colony stimulating factor (M-CSF) and receptor activator of nuclear factor-κB ligand (RANKL)-induced osteoclastogenesis. Additionally, the VnP-8-DN1 dimer increased the survival of bone marrow-derived macrophages and decreased the cellular level of c-Fms, a cell surface receptor of M-CSF, after which it reduced the expression level of receptor activator of nuclear factor-κB. These findings indicated that the VnP-8-DN1 dimer affected M-CSF signaling and blocked mitogen-activated protein kinase signaling induced by M-CSF or RANKL, which is critical for osteoclast differentiation. A pull-down assay using biotinylated VnP-8-DN1 dimers demonstrated that the peptide was associated with c-Fms, indicating that the VnP-8-DN1 dimer inhibits M-CSF and RANKL-induced osteoclastogenesis via c-Fms. Overall, these results highlight the potential applicability of the VnP-8-DN1 dimer as a bone disease and bone regeneration therapeutic agent by regulating osteoclast differentiation.

**Keywords:** IDAAFTRINCQG motif, 11-mer dimeric peptide, Cell behavior, Osteoclastogenesis, c-Fms, Bone regeneration

***Student Number*:** 2016-36909

# CONTENTS

# BACKGROUND

## 1. Bioactive peptides for bone regeneration

The optimal approach to regenerate damaged bone tissues is to recreate an organized environment similar to that of the native tissue. In other words, the artificial surroundings of the cells should be made similar to their normal environment. Tissue regeneration requires the supply of scaffolds, tissue cells, and biochemical factors to provide the appropriate environment for cell growth [1]. As a source of these essential factors, extracellular matrix (ECM) proteins play a significant role in structural tissue support and biological processes such as cell attachment, migration, proliferation, and differentiation [2]. Biological scaffolds facilitate the effective settlement of transplanted cells in the damaged tissue and play a significant role in inducing tissue cells to efficiently regenerate the damaged tissue while also providing adequate structural support [3,4]. In damaged tissue, the specific cells quickly attach to a substrate, such as a scaffold, inducing proliferation and differentiation for tissue regeneration [5]. However, bone cells do not attach strongly to most biodegradable synthetic polymers [6]. Thus, the modification of biomaterial scaffolds with appropriate bioactive peptides for improved attachment could further strengthen the bone regenerative functions of the cells [7,8]. Biological scaffolds composed of ECM components are useful for tissue engineering applications. ECM-derived peptides provide effective surface functions for the control of cellular behaviors. Many studies have identified bioactive peptides using ECM proteins

such as collagen [9], fibronectin [10], and laminin [11,12]. Peptides containing RGD sequences are known to be important components of ECM adhesive proteins and are widely used for biomaterial modification [13,14]. In a rat model, peptides derived from laminin immobilized to titanium scaffolds promoted bone regeneration through osteoblast function improvement, indicating that the modification of the surface of a scaffold with appropriate bioactive peptides could lead to the enhancement of their cellular activity and functions [15]. Moreover, the promotion of cell attachment and other specific functions using integrin- or heparin-binding peptides has also been extensively studied. The heparin-binding peptide, corresponding to residues 15-24 of BMP-4 induced differentiation of human mesenchymal stem cells into osteoblastic cells by phosphorylating ERK1/2 (i.e., an extracellular signal-regulated kinase) [16]. Moreover, VnP-16, a β1 integrin-binding peptide, was found to promote bone regeneration by stimulating osteogenic differentiation and inhibiting osteoclast differentiation [17]. Taken together, these observations highlight the applicability of ECM protein- or cytokine-derived peptides as promising therapeutic tools for tissue regeneration.

## 2. Osteoclast differentiation and bone defect

Osteoclasts are bone tissue-specific, tartrate-resistant, acid phosphatase (TRAP)-positive multinuclear cells that resorb bone and differentiate from hematopoietic cell monocyte/macrophage lineages [18]. Osteoclast differentiation and function require two major cytokines: the macrophage-colony stimulating factor (M-CSF) and the receptor activator of nuclear factor-κB ligand (RANKL) [19,20]. M-CSF- or RANKL-deficient mice result in a severe osteopetrotic phenotype owing to osteoclast-forming and bone-

resorbing impairment, indicating that M-CSF or RANKL signaling is crucial for osteoclast formation [21,22]. During the osteoclast formation process, bone marrow precursor cells undergo several stages including the proliferation of fusion-competent cells, mononuclear preosteoclast fusion, and osteoclast maturation, all of which ultimately results in terminally differentiated bone-matrix-degrading osteoclasts [23]. Therefore, the treatment of osteoclast-related diseases often relies on blocking signal transduction pathways involved in osteoclast formation and bone resorption at each stage of osteoclast differentiation.

In pathological conditions such as inflammation and steroid hormone deficiencies, abnormal bone resorption results in abnormal bone remodeling and development of bone disorders [24]. Increases in osteoclast-mediated bone resorption can lead to impaired bone structure and bone loss conditions such as osteoporosis, rheumatoid arthritis, Paget's disease, and metastatic bone disease [23,25,26].

## 3. Bioactive peptides as therapeutic agents for bone disease

Osteoclast-related diseases are mainly treated using bisphosphonates, denosumab, and estrogen therapy. However, these treatments invariably lead to multiple side-effects or even exacerbate health problems with long-term use [27]. Therefore, further research is necessary to identify potential clinical candidates and improve the pharmacological and therapeutic alternatives for osteoclast-related disease treatment. Regeneration of bone defects derived from injury or disease can be approached by controlling cell behaviors using bioactive peptides [28]. Developing a peptide that mimics the active site of a native protein would allow for the specific regulation of osteoclast differentiation

and resorption-related signals with the added advantages of cost-efficiency, immunogenicity, and high specificity [29,30]. Thus, bioactive peptides can be used as useful tools to block key signaling pathways associated with osteoclast differentiation or activation. A previous study demonstrated that WP9QY, a tumor necrosis factor (TNF) receptor mimetic peptide, blocked bone resorption activity of osteoclasts by interfering with both RANKL and TNF-induced osteoclast recruitment and activation [31]. The cell-permeable peptide, receptor activator of nuclear factor-κB (RANK) receptor inhibitor (RRI) peptide has also been reported to inhibit osteoclast formation and bone loss targeting a specific RANK signaling by acting at the terminal differentiation stage of osteoclastogenesis [32].

# INTRODUCTION

Several tissue engineering techniques have been developed and utilized for the regeneration of trauma- or disease-damaged bone tissue. Particularly, effective tissue regeneration can be achieved by rapidly eliciting cell reactions around the damaged area, thereby improving the scaffold's surface properties as a biological supporter using physical and chemical methods [33]. This approach has been applied for scaffold surface modification using several adhesive extracellular matrix proteins, including collagen, fibronectin, and laminin, as well as several growth factors such as bone morphogenetic protein 2 and fibroblast growth factors [28,34,35]. However, native or recombinant proteins used in regenerative medicine can be extremely costly and induce undesirable immune responses resulting in reduced efficacy, anaphylaxis, and autoimmunity. Moreover, due to their short half-life and diffusion from the regenerative site, high doses of these proteins are frequently required, which causes further side effects [36,37]. An alternative and more efficient approach is to utilize a relatively short peptide derived from the active domains of the ECM proteins to induce cell attachment and specific cell functions. Peptides have several advantages over entire proteins in therapeutic applications such as their low cost, low toxicity, limited immunogenicity, structural variety, and functional flexibility [29,38]. Importantly, bioactive peptides have been studied to partially or equally mimic the effects of native proteins on diverse cellular responses such as cell attachment, spreading, migration, proliferation, and differentiation.

Bone tissue is maintained via remodeling and reconstruction through the interaction

of osteoblasts forming bone and osteoclasts resorbing bone [39]. Chronic inflammatory diseases such as periodontitis and arthritis cause osteoclasts abundance or excessive bone absorption due to increased inflammatory substances, leading to bone loss [24,25,40]. Osteoclast differentiation and activity are regulated via the stimulation of various signaling proteins such as MAPKs, including ERK, JNK, and P38. Additionally, M-CSF induces the activation of phosphoinositide 3-kinase and mitogen-activated protein kinases (MAPKs) in association with the c-Fms, its receptor [41] and mediates the survival and proliferation of osteoclast precursors, as well as osteoclast differentiation. RANKL binds to RANK and also activates MAPKs through the recruitment of a TNF family protein such as TRAF6, and activates transcription factors such as c-Fos and NFATc1 to promote the fusion and maturation of mononucleated cells into multinucleated TRAP-positive cells. Additionally, RANKL/RANK signals induce the expression of proteins such as integrin αβ3 and cathepsin K, thereby regulating substrate absorption capacity [23,42,43]. Many studies have demonstrated the potential therapeutic applicability of peptides as modulators of osteoclast differentiation [44,45].

Vitronectin is an adhesive, multifunctional glycoprotein that existed in bone matrix and plasma, and is known to mediate cell adhesion, spreading, migration, immune responses, and blood clotting [46,47]. Moreover, vitronectin is thought to be involved in bone metabolism, as it occurs in large amounts in the bone matrix [48]. Vitronectin comprises four structurally distinct domains: a somatomedin domain, hemopexin-like domains, and a connecting region that bridges the somatomedin and hemopexin-like domain 1. Among them, hemopexin-like domains are also found in most members of the matrix metalloproteinases family [49] and enable the binding to a variety of molecules

and proteins [50]. Particularly, heparin-binding sequences in hemopexin-like domains are known to mediate various cellular responses [51,52]. Therefore, it is possible to improve overall bone regeneration ability by inducing a rapid cellular response to tissue-specific cells by identifying an active peptide that promotes vitronectin-induced cell attachment.

The aim of this study was to identify bioactive peptides within human vitronectin and to evaluate the effect of peptides on osteoclast differentiation and its molecular mechanisms. This study identified VnP-8-DN1, a functional dimeric peptide with heparin-binding activity, which was found to promote cell attachment and chondrogenic differentiation while also inhibiting osteoclast differentiation. Additionally, this VnP-8-DN1 dimer was found to inhibit osteoclast differentiation both in soluble form in culture medium and immobilized in a culture dish. Particularly, the peptide inhibited osteoclast differentiation, which occurred via c-Fms association, leading to the inhibition of M-CSF-induced MAPKs activation and downregulation of RANK expression.

# MATERIALS AND METHODS

## Peptides and reagents

Peptides were prepared by the 9-fluorenylmethoxycarbonyl-based solid-phase peptide synthesis using an ASP48S (Peptron Inc., Korea) and modified with a C-terminal amidation. The peptides were purified by the reverse-phase high-performance liquid chromatography (Shimadzu Prominence HPLC, Japan) using a Vydac Everest C18 column, 250 mm × 22 mm, 10 μm (Hichrom, Berkshire, UK) and eluted with a water-acetonitrile linear gradient (10~75% (v/v) of acetonitrile) containing 0.1% (v/v) Trifluoroacetic acid. For the homodimer reaction, the monomeric peptide was dissolved in water-acetonitrile solution (50/50, v/v) to 10 mg/ml concentration with a vigorous stir and added saturated ammonium acetate solution to adjust pH 8.0. The progress of the reaction was monitored by Elman's reagent. Molecular weights on the purified peptide were determined using liquid chromatography–mass spectrometry (Shimadzu LC/MS-2020 series, Japan). All procedures were carried out by Peptron (Daejeon, Korea). All peptides used in the study were more than 93% purity.

M-CSF and RANKL are obtained from PEPROTECH KOREA. Antibodies specific for NFATc, c-Src, p-CREB, Integrin αv, β3, p-ERK, ERK, p-JNK, JNK, p-p38, and p38 were purchased from Cell signaling (Boston, MA, USA). Anti-RANK, TRAF6 and c-Fos were obtained from Santa Cruz Biotechnology (Dallas, TX, USA); and actin was from Sigma Aldrich (St. Louis, MO, USA).

## Design of the synthetic peptides

The strategy for biologically active peptide screening was based on the overlapping peptide synthesis of the entire protein sequence [53], which is then individually tested for binding to the specific cells, searching the identification of peptide-binding receptors or molecules. Based on this method, ten overlapping peptides covering amino acid residue 150-233 of the hemopexin-like domain 1 were prepared.

## Cells and cell culture

Human skin-derived precursors (SKPs) were used to differentiate into osteogenic cells as described previously [54]. Briefly, the SKPs were isolated from human foreskin, and then differentiated into mesenchymal precursors. For differentiation into osteogenic cells, The mesenchymal precursors cultured in α-MEM supplemented with 10 mM β-glycerol phosphate, 10 μM dexamethasone, 200 μM ascorbic acid, and 10% FBS for 2 weeks. Human osteosarcoma (HOS) cells were maintained in Dulbecco's modified Eagle's medium (DMEM, Invitrogen, Carlsbad, CA, USA) supplemented with antibiotics and 10% fetal bovine serum (FBS, Invitrogen). ATDC5 cell, a murine chondrogenic cell line, was cultured in α-MEM supplemented with antibiotics and 5% FBS. Bone marrow-derived cells were isolated from the tibiae and femurs of 6-7 week-old female C57BL/6 mice by flushing of the bone marrow cavity. After removing erythrocytes by treatment with ACK buffer (0.01 mM EDTA, 0.011 M $KHCO_3$, and 0.155 M $NH_4Cl$, pH 7.3), and the cells were cultured with α–minimum essential medium (α-MEM; Invitrogen), 100 U/ml penicillin, 100 μg/ml streptomycin, and 10 ng/ml M-CSF under a humidified atmosphere of 5% $CO_2$ at 37°C for 12 h. Non-adherent floating cells were incubated with

30 ng/ml M-CSF for further 3-5 days until 80% confluent. These stage cells were regarded to be bone marrow macrophages (BMMs) and used as osteoclast precursors. All procedures for obtaining animal specimens were approved by the Ethics Committee at Institutional Animal Care and Use Committee (approval number: SNU-180517-1-1).

## Preparation of peptide stock solutions

Peptides were dissolved in double-distilled water (DDW) or dimethyl sulfoxide (DMSO) at the concentration of 1 mg/ml, and then briefly sonicated for 10 seconds 3 times. In the case of the insoluble peptide, dissolved the peptide in the smallest possible volume of 10% (v/v) DMSO in water and subsequently add water until the concentration is 1 mg/ml.

## Spontaneous air oxidation reaction of peptide

The peptides were dissolved in DDW to prepare 5 mg/ml peptide solutions in the tubes were gently spun with a rotator (Model 7637, COLE-PARMER, USA) at room temperature for 9 hours per day, stored at -20°C for the rest of the day, and then repeated next day. The molecular weight of each peptide was analyzed by high-performance liquid chromatography (HPLC) and mass spectrometry.

## Cell attachment and spreading assays

Cell attachment assays were performed as described previously [54]. Briefly, for peptide immobilization on the plate, peptides were loaded into 48-well culture plates at an indicated concentration and followed to be adsorbed onto the plates by air drying for

18 h at room temperature. The concentrations of synthetic peptides were determined from a dose–response curve, and the lowest concentration achieved maximum attachment to the cells was used Human plasma vitronectin was used at a concentration of 1 ug/ml following the manufacturer's instructions. Experiments were conducted with 9.1 μg/cm$^2$ peptide coating concentrations based on the earlier study performed with VnP-16 peptide [17]. Peptide-coated plates were blocked with 1% heat-inactivated bovine serum albumin (BSA; Gibco BRL) in phosphate-buffered saline (PBS) for 1 h at 37°C, and then washed with PBS. Cells ($5 \times 10^4$ cells/250 μl) were seeded to each well and attached for 1 h at 37°C. After incubation, the unattached cells were removed and washed the plates once with PBS. The attached cells were fixed with 10% formalin for 15 min and stained with 0.5% crystal violet for 1 h. The plates were gently washed with DDW three times and the stained cells were dissolved in 2% sodium dodecyl sulfate (SDS) for 5 min. The absorbance was assessed at 570 nm using a microplate reader (Bio-Rad). For cell spreading assay, cells were seeded on each peptide-coated plate at a density of $3 \times 10^4$ cells/250 μl and incubated for 3 h at 37°C. After staining cells, the area of the cell surface was imaged and analyzed using Image-Pro plus software (Media Cybernetics, Silver Spring, MD). At least 100 cells were analyzed on each well.

## Attachment inhibition assay

Cells were pretreatment for 15 min in serum free medium containing 5 mM EDTA or 100 μg/ml heparin. The pretreated cells were seeded on peptide-coated plates and further incubated for 1 h. Attached cells were stained with 1% crystal violet, and then dissolved in 5% SDS for 5 min and quantified by the optical density at absorbance at 570

nm using a microplate reader (Bio-Rad).

## Chondrogenic differentiation assay

Passage number 3-5 of ATDC5 cells were seeded at a density of 4 x $10^5$ on 24-well plate and grown to 120% confluency in growth medium DMEM/F12 medium supplemented with 5% fetal bovine serum (FBS), 100 U/mL penicillin, and 100 μg/mL streptomycin. And then, the cells cultured in differentiation medium supplemented with 1% insulin transferrin and selenium in a humidified incubator with 5% $CO_2$ at 37°C for 7 days or 14 days. The differentiation medium was changed every second or third day. To assess chondrogenic differentiation, Alcian blue staining was performed. Cells were fixed in 4% paraformaldehyde for 20 min and stained with 1% Alcian blue 8GX in 0.1 M hydrochloric acid for 1 h. Cells were washed in DDW three times, and images were photographed.

## Quantitative real-time PCR

For quantitative real-time polymerase chain reaction (qRT-PCR) analysis, total RNA was isolated from the cells using the RNeasy Mini Kit (Qiagen, Valencia, CA, USA) following the manufacture's instruction. The cDNA was prepared from 2 μg of RNA using SuperScript™ III Reverse Transcriptase (Invitrogen). The qRT-PCR was performed with SYBR® Green PCR Master Mix (TaKaRa) and conducted using a 7500 Real-time PCR System (Applied Biosystems). The PCR reaction was performed for 30 s at 95°C, followed by 40 amplification cycles (15 s at 95°C, 30 s at 60°C, 35 s at 72°C). Relative expression levels for each gene were expressed as fold changes by the $2^{-\Delta\Delta Ct}$ method [55].

Aggrecan and col2a1 primers were designed using Primer Express 3.0.1 software (Thermo Fischer Scientific) as follows: forward for aggrecan, 5'- GCT GCC CTT CAC GTG TAA AAA -3', and reverse for aggrecan, 5'- CTG ATC TCG TAG CGA TCT TTC TTC T -3'; forward for col2a1, 5'-GTA AAC TTG GGC ACT TTG TGG AA-3', and reverse for col2a1, 5'-TGA TGA TGT AAC CTA CGT CAG GTG TT-3'

## Osteoclast differentiation assay

To generate mouse bone marrow-derived osteoclasts, Bone marrow macrophages (BMMs; $1 \times 10^5$ cells/48-well culture plate) were cultured on 48 well plate in a α–minimum essential medium (α-MEM; Invitrogen) containing 100 U/ml penicillin, 100 μg/ml streptomycin, 30 ng/ml M-CSF, and 100 ng/ml recombinant murine RANKL for 4 days. Peptides were prepared at a concentration of 5 mg/ml stock solutions. The differentiation medium was changed after culture on day 3. The differentiated cells were fixed with 4% paraformaldehyde and stained for TRAP, using the Leukocyte Acid Phosphatase Assay Kit (Sigma-Aldrich) according to the manufacturer's instructions. TRAP-positive multinucleated cells with more than three nuclei were regarded as osteoclasts.

## Bone resorption assay *in vitro*

Resorption assays were performed using Osteo Assay Surface as described previously [17]. Mouse BMMs were cultured on Osteo Assay Surface plates (Corning) for 4 days with differentiation medium containing M-CSF (30 ng/ml) and RANKL (100

ng/ml) in the presence of peptides. After incubation, the medium was aspirated and washed with PBS. Then, the cells were removed using 10% Clorox (0.56% NaOCl), then washed with DDW twice and air-dried. The resorption areas were captured and analyzed using the Image Pro-Plus program (version 4.0; Media Cybernetics).

## Western blot analysis

Mouse bone marrow macrophages ($1 \times 10^6$) were seeded on 35 mm culture dishes with 50 μg/ml monomeric or dimeric peptide and incubated for the indicated times. The cells were then washed with ice-cold PBS and suspended with 150 μl RIPA buffer (50 mM Tris-HCl, pH 7.4, 150 mM NaCl,1 mM EDTA, 1% Triton X-100, 1 mM PMSF, 2 mM $Na_3VO_4$, and 1 mM glycerol phosphate) containing a protease and phosphatase inhibitor cocktail (Roche). The protein lysates were centrifuged at 10,000 × g for 15 min at 4°C, after which the protein concentration was measured using BCA assay kit (Thermo scientific). Proteins were denatured using SDS sample buffer. After SDS-PAGE, separated proteins were transferred to nitrocellulose membranes. The membranes were immunoblotted with primary antibodies against MAPKs, c-Fos monoclonal antibody, and anti-NFATc1, anti-c-Src, anti-p-CREB, anti-integrin $\alpha$v, anti-integrin β3, and anti-$\beta$ actin polyclonal antibody, then probed with anti-rabbit horseradish peroxidase-conjugated secondary antibodies (Cell Signaling Technology, Danvers, MA, USA). The signals were detected by chemi-luminescence device. The ratio of $\beta$-actin against all target proteins was used as a loading control.

## Pull-down assay using biotin-conjugated peptide

Pull-down assays were performed as in a previous report [56] using biotin-conjugated VnP-8-DN1 monomeric and dimeric peptides. Cells ($1 \times 10^7$ cells) were seeded on 100-mm dishes and incubated for 2 days in growth medium containing 30 ng/ml M-CSF and washed twice with cold PBS. Cells were scraped with 500 μl lysis buffer (50 mM Tris-HCl, pH 7.5, 150 mM NaCl, 0.1% sodium deoxycholate, 1% Triton X-100) containing protease inhibitor cocktail tablets (Roche) and homogenized by passing the lysate 15 times through a 26.5-gauge needle, followed by centrifugation at 17,000 × g for 15 min at 4°C. The supernatants were mixed with biotin-conjugated peptides (50 μg/ml) for 2 h and dissolved in 50 μl of streptavidin agarose beads (Thermo Scientific, Rockford, IL, USA) for 16 h at 4 °C and centrifuged at 1,500 × g for 2 min at 4°C. After washing the beads pellet four times with lysis buffer, the precipitated proteins were fractionated by 8.5% or 10% SDS-PAGE and analyzed by immunoblotting.

## Immunostaining

BMMs were seeded on 4-well chamber slide (Lab-Tek) in a medium containing 50 μg/ml of peptides for 4 days. After the cells were washed with PBS twice, fixed with 3.7% paraformaldehyde in PBS for 20 min, and permeabilized with 0.5% Triton x-100 in PBS for 5 min at room temperature. The fixed cells were blocked with 1% BSA in PBS for 1 h and probed with anti-phalloidin conjugated rhodamine for 18 h at 4°C. The chamber slide was mounted using coverslip glass with fluorescent mounting medium, observed under a Zeiss LSM700 confocal fluorescence microscope and photographed by CDD camera.

## Cell viability assay

For cell viability analysis of bone-marrow macrophages, the EZ-Cytox cell viability assay kit was used. BMMs were seeded on 48-well culture plate at a density of $1 \times 10^5$ cells/ in a 1 ml volume per well, and allowed to culture for the indicated times with the presence or absence of M-CSF (30 ng/ml) or the peptide (50 μg/ml). After incubation, 100 μl of water-soluble tetrazolium solution was added in each well and further incubation for 2 or 4 h. The absorbance was measured by a microplate reader at 450 nm (Bio-Rad, USA).

## Statistical analysis

All data were expressed as the mean ± SD. The data were analyzed by analysis of variance (ANOVA). When significant differences between groups were found, pairwise comparisons were conducted using Scheffé's adjustment. Statistical significance was determined using a Student's t-test. *P* value of 0.05 was considered significant.

# RESULTS

## Effects of vitronectin-derived peptides on osteogenic cell attachment

As shown in Fig. 1, a series of overlapping 12-mer peptides (VnP-1 to VnP-10) covering the hemopexin-like domain 1 in human vitronectin (amino acids 150–233) was synthesized. A cell attachment assay was then performed to identify functional bioactive peptides in synthetic peptide-coated plates. A dose-response curve was calculated to determine the optimal synthetic peptide concentration, and the lowest concentration to which human osteogenic cells were maximally attached was used [17]. To clarify the cell-attachment-promoting activity of peptides, cell attachment assays were conducted with 10.9 μg/cm$^2$ peptide levels. Human osteogenic cells differentiated from skin-derived precursors (SKPs) were used to test cell attachment activity to the synthetic peptides [57]. When the peptides were used immediately after preparation of the stock solution, VnP-4 (AFRGQYCYELDE, residues 174-185), VnP-6 (PGYPKLIRDVWG, residues 190-201), and VnP-8 (IDAAFTRINCQG, residues 206-217) exhibited cell attachment activity (Fig. 2A), and VnP-8-coated plates exhibited increased cell attachment in a dose-dependent manner and peaked at a concentration of 10.9 μg/cm$^2$ (50 μg/ml, Fig. 2B). However, uneven seeding patterns in the culture plate were observed in VnP-4 and VnP-8-coated dishes, which translated to considerable data variations. These variations might have been due to poor peptide solubility. To overcome this problem, peptide stock solutions were briefly sonicated. After sonication, VnP-8 exhibited strong cell attachment activity similar to that of vitronectin and displayed even seeding patterns in culture plates (Fig.

2C); however, VnP-4 had a weak cell-binding activity. However, the rest of the peptides except VnP-8 and VnP-4 showed no cell attachment activity. The VnP-8 sequence is conserved in rat, mouse, and human vitronectin. Recent reports show that the DAAFT sequence in VnP-8 maps to the β-strand of hemopexin-like domain 2 of vitronectin (Fig. 1) [58]. Taken together, these results demonstrate that VnP-8 promotes cell attachment activity.

## Morphological changes in cells attached to VnP-8 exposed to air

VnP-8 exhibited strong cell attachment activity (Fig. 2C), but cells attached to the VnP-8-coated plate showed morphological differences in each experiment (data not shown). This phenomenon is presumed to result from the modification of peptide structure or sequence, which is the result of spontaneous air oxidation during the preparation of the peptide solution. Therefore, it was confirmed that there was a difference in the morphology of the attached cells using peptides that were stored at room temperature for 1 day, 5 days and 1 month. It has been observed that the longer the peptide is exposed to air, the more stable and well spread the cells are (Fig. 3). These results suggest that some modified VnP-8 peptide sequences can enhance cell attachment activity.

## VnP-8 peptide profiles modified by spontaneous air oxidation

VnP-8 contains a cysteine residue in its sequence and therefore can easily oxidize when exposed to air and forms a dimerization link via a disulfide bond between two cysteine residues [59]. To clarify the effect of different air oxidation times on peptide

modification, VnP-8 stock solutions (5 mg/ml) were stored at room temperature for 5 days, 1 month, or 3 months. Mass spectrometry analysis showed that the VnP-8 monomers were mostly changed to dimeric form. Various dimerized VnP-8 peaks were found in all tested VnP-8 stock solutions (Fig. 4B), demonstrating that most of the monomeric state, which was an original form of VnP-8, was modified to a dimeric state. We speculate that isoleucine was removed at the N-terminus of VnP-8, and disulfide bonds were formed between the two cysteine residues (Fig. 4A). These findings indicate that the dimeric form of VnP-8 may contribute to improved cell attachment.

## Dimeric peptide converted from VnP-8 enhances cell attachment activity

Synthetic VnP-8 dimers and VnP-8-DN1 dimers were prepared to evaluate the cell attachment activity of the dimeric peptides formed by air oxidation. Osteogenic cells were cultured on VnP-8-, VnP-8 dimer-, VnP-8-DN1 monomer-, and VnP-8-DN1 dimer-coated plates in serum-free medium for predetermined times. The VnP-8-DN1 dimer enhanced cell attachment faster than other peptides 7 min after seeding and exhibited the highest attachment activity among the other peptides over 3 h (Fig. 5). Overall, VnP-8-DN1 dimer showed higher cell attachment activity than monomeric peptides; therefore, downstream experiments were conducted with the VnP-8-DN1 dimer as the bioactive peptide.

### VnP-8-DN1 dimer promotes osteogenic cell attachment and spreading

Given that VnP-8-DN1 dimer scrambled peptides could not be synthesized, the VnP-8-DN1 monomer was used as a negative control for downstream experiments. Cell

attachment to the VnP-8-DN1 dimer increased in a dose-dependent manner and reached a maximum at a concentration of 2.1 μg/cm$^2$ (Fig. 6A). The cell attachment level achieved with the VnP-8-DN1 dimer was similar to that of vitronectin (Fig. 6B). However, cell attachment was largely unaffected by BSA and the VnP-8-DN1 monomer. Additionally, the cell spreading activity of the Vn8-DN1 dimer increased approximately 4 times compared to the VnP-8-DN1 monomer and BSA negative controls (Fig. 6C). These results demonstrate that the VnP-8-DN1 dimer promotes cell attachment and spreading in osteogenic cells.

**VnP-8-DN1 dimer mediates cell attachment by heparin-binding activity**

Attachment of cells to ECM proteins is mainly mediated by integrins or heparan sulfate proteoglycans such as syndecans and glypicans [60]. Proteoglycans consist of core proteins and glycosaminoglycans, which contain linear, anionic, sulfated polysaccharides [61]. Heparin, which is a type of glycosaminoglycan is widely used as a model reagent of heparan sulfate. Integrin binding to their ligands requires a divalent cation and is inhibited by EDTA, a metal chelating reagent [62]. Therefore, the effect of heparin or EDTA as competitors during cell attachment was investigated to determine the cellular receptor properties involved in the VnP-8-DN1 dimer binding process. Heparin significantly inhibited cell attachment of osteogenic cells to VnP-8-DN1 dimers compared to the vehicle (Fig. 7A), suggesting that the VnP-8-DN1 dimer mainly interacted with heparan sulfate proteoglycan receptors. Pretreatment of cells with EDTA also slightly inhibited cell attachment to the VnP-8-DN1 dimer, indicating that VnP-8-DN1 dimer-mediated attachment is partially involved in cation-dependent receptors such

as integrins or α-dystroglycans. Additionally, the binding between heparin and VnP-8-DN1 dimer was confirmed via a solid-phase heparin binding assay. Compared to the VnP-8-DN1 monomer, the VnP-8-DN1 dimer exhibited high heparin-binding activity in a dose-dependent manner (Fig. 7B). These findings suggest that the heparin-binding activity of the peptide is critical during VnP-8-DN1 dimer-mediated cell attachment.

**VnP-8-DN1 dimer promotes attachment of ATDC5 cells and induces chondrogenic differentiation**

The heparin-binding domain has been implicated as an important modulator of osteoblast differentiation and activity [63,64]. Therefore, the effect of the VnP-8-DN1 dimer with heparin-binding activity on chondrogenic cell behavior or chondrocyte differentiation was investigated. The VnP-8-DN1 dimer promoted the cell attachment of chondrogenic ATDC5 cells to a level that was comparable to that of vitronectin (Fig. 8A). Afterward, to assess the effects of the VnP-8-DN1 dimer on chondrogenesis, chondrocyte precursor ATDC5 cells were cultured in chondrogenic differentiation medium containing VnP-DN1 dimer for 14 days. ATDC5 cells are known to differentiate into chondrocytes in the presence of 1X insulin-transferrin-sodium selenite (ITS) [65]. Even in the absence of ITS, the VnP-8-DN1 dimer increased proteoglycan deposition in alcian blue staining (Fig. 8B). Next, to assess the expression levels of chondrogenic markers, cells were cultured in differentiation medium treated with BMP-2, VnP-8-DN1 dimer, or BMP-2 + VnP-8-DN1 dimer for 7 days. The VnP-8-DN1 dimer alone significantly increased the expression of the chondrogenic marker genes aggrecan and col2α1 compared to untreated cells (Fig. 8C). Additionally, in the presence of BMP-2, VnP-8-DN1 dimer

synergistically induced the chondrogenic effect of BMP-2 (Fig. 8C). These results suggest that the VnP-8-DN1 dimer induces ATDC5 cell attachment and cell chondrogenic differentiation.

**VnP-8-DN1 dimer suppresses M-CSF and RANKL-induced osteoclastogenesis**

The heparin-binding domain of proline/arginine-rich end leucine-rich repeat protein (PRELP) was reported to act as a cell type-specific NF-κB inhibitor that impairs osteoclastogenesis [66,67]. To examine the effect of the VnP-8-DN1 dimer on osteoclast differentiation, BMMs were differentiated into osteoclasts onto VnP-8-DN1 dimer-coated plates in the presence of M-CSF and RANKL. M-CSF and RANKL induced the formation of numerous TRAP-positive multinucleated osteoclasts from BMMs. The VnP-8-DN1 dimer almost completely inhibited M-CSF and RANKL-induced osteoclastogenesis, whereas the vehicle and the VnP-8-DN1 monomer had no effect (Fig. 9A, B). Furthermore, the average size of the M-CSF and RANKL-induced osteoclasts was reduced by the VnP-8-DN1 dimer (Fig. 9A, C). Additionally, when used at the concentration that blocked osteoclastogenesis (9.1 $\mu g/cm^2$), the VnP-8-DN1 dimer did not affect the proliferation or viability of BMMs (Fig. 9D), indicating that its inhibitory effect on osteoclastogenesis was not due to cytotoxicity or reduced cell proliferation.

When the VnP-8-DN1 dimer was coated onto the culture plate, M-CSF and RANKL-induced osteoclastogenesis was inhibited, thereby confirming whether the peptide had the same effect when treated to the culture medium. To assess this, BMMs were differentiated into osteoclasts with the VnP-8-DN1 dimer in the presence of M-CSF (30 ng/ml) and RANKL (100 ng/ml) for 4 days. The VnP-DN1 dimer significantly

reduced the formation of TRAP-positive multinucleated osteoclasts (Fig. 10A, B). In contrast, the VnP-8-DN1 monomer had no inhibitory effect on osteoclast formation. In addition to the number of osteoclasts, the average size of the M-CSF and RANKL-induced osteoclasts was reduced by the VnP-8-DN1 dimer compared to that of the vehicle or the VnP-8-DN1 monomer. To further confirm the inhibitory effect of the VnP-8-DN1 dimer on osteoclast differentiation, the expression of osteoclastogenesis-related proteins was examined at days 0, 1, 2, and 3. c-Fos, NFATc1, and ATF-1 are key transcription factors during osteoclastogenesis, which are molecules downstream of NF-kB and are upregulated by activation of MAPKs [42,68]. As shown in Fig. 11, RANKL and M-CSF induced c-Fos and NFATc1 expression and phosphorylation of ATF-1. Moreover, the VnP-8-DN1 dimer inhibited the expression of c-Fos and NFATc1 and activation of ATF-1, whereas the VnP-8-DN1 monomer did not inhibit their expression levels. Additionally, the VnP-8-DN1 dimer completely blocked the expression of integrins αv and β3, which have a critical role in osteoclast precursor fusion and maturation. c-Src, an upstream regulator of p38, was also suppressed by the VnP-8-DN1 dimer. The anti-osteoclastogenic effects of the VnP-8-DN1 dimer were confirmed by its ability to suppress F-actin-mediated cytoskeletal organization in BMMs (Fig. 12A). Afterward, to investigate whether the VnP-8-DN1 dimer affected bone-resorbing activity *in vitro*, BMMs were cultured for 4 days on vehicle-, VnP-8-DN1 monomer-, or VnP-8-DN1 dimer-coated Osteo Assay Surface plates in the presence of M-CSF and RANKL. The VnP-8-DN1 dimer significantly inhibited the number and area of these resorption pits (Fig. 12B), demonstrating that it could inhibit bone resorption as a result of osteoclast differentiation suppression. These results indicate that the VnP-8-DN1 dimer

suppresses osteoclast differentiation.

**VnP-8-DN1 dimer blocks the initial stage of M-CSF and RANKL-induced osteoclastogenesis**

Osteoclast precursors undergo multiple stages during osteoclast differentiation. To determine the stage of osteoclast differentiation at which the VnP-8-DN1 dimer acts, BMMs were treated with the VnP-8-DN1 dimer for the indicated times in the presence of M-CSF (30 ng/ml) and RANKL (100 ng/ml) for 4 days and examined osteoclast formation. The VnP-8-DN1 dimer showed strong anti-osteoclastogenic effects on days 1, 2, and 3. On the other hand, VnP-8-DN1 dimer treatment had no significant effect on osteoclast differentiation during the last 3 days (Fig. 13), indicating that VnP-8-DN1 dimer treatment for the first day was sufficient to inhibit osteoclast differentiation during osteoclastogenesis. These results indicate that the VnP-8-DN1 dimer acts as an inhibitor in the early stages of osteoclastogenesis.

**VnP-8-DN1 dimer suppresses M-CSF or RANKL-induced signaling**

MAPKs, including ERK, JNK, and p38, are activated by M-CSF or RANKL in BMMs, and regulate downstream target molecules such as c-Fos and NFATc1, all of which are critical factors for osteoclast differentiation [43,68,69]. To explore whether the VnP-8-DN1 dimer affects the signaling pathway stimulated by M-CSF or RANKL, MAPK-mediated activations were analyzed. ERK, JNK, and p38 were activated by M-CSF and RANKL, and the VnP-8-DN1 dimer significantly attenuated the M-CSF-induced activation of these MAPKs (Fig. 14A). Moreover, the VnP-8-DN1 dimer

inhibited RANKL-induced activation of MAPKs in BMMs (Fig. 14B). These results suggest that the VnP-8-DN1 dimer inhibits activation of ERK, JNK, and p38 induced by both RANKL and M-CSF.

**Effects of VnP-8-DN1 dimer on the viability of BMMs and c-Fms and RANK levels**

Given that the VnP-8-DN1 dimer inhibited M-CSF-induced MAPK activation, the effects of the VnP-8-DN1 dimer on the survival and proliferation of osteoclast precursors (i.e., a biological function of M-CSF) were further examined. M-CSF promotes the survival and proliferation of osteoclast precursors and organizes osteoclast cytoskeletons [20,70]. BMMs treated with the VnP-8-DN1 dimer were cultured for 24, 48, and 72 h in the presence or absence of M-CSF. As expected, the absence of M-CSF dramatically decreased the cell viability of BMMs in a time-dependent manner (Fig. 15A). However, the VnP-8-DN1 dimer enhanced cell viability compared to the vehicle in the absence of M-CSF. In the presence of M-CSF, VnP-8-DN1 reduced cell proliferation compared to M-CSF alone. These results indicate that the inhibition of BMM proliferation and the low cell survival levels induced by the VnP-8-DN1 dimer may be attributed to M-CSF signaling malfunction.

Additionally, RANKL provides the signals required for the differentiation of osteoclast precursors by binding to its receptor (RANK) [71]. To investigate the inhibitory mechanisms of the VnP-8-DN1 dimer on osteoclast differentiation, the expression of these receptors in the presence of the VnP-8-DN1 dimer was analyzed 24 h after peptide treatment. The level of c-Fms in BMMs was downregulated by either M-CSF or the VnP-8-DN1 dimer; however, M-CSF induced RANK expression in BMMs,

whereas the VnP-8-DN1 dimer decreased RANK expression (Fig. 15B). These results suggest that c-Fms is degraded by treatment with VnP-8-DN1 dimer, leading to the reduction of RANK expression.

**VnP-8-DN1 dimer associates with c-Fms**

Given that the levels of c-Fms and cell survival were altered by the VnP-8-DN1 dimer, this study investigated whether the nP-8-DN1 dimer interacts with c-Fms. BMMs were cultured on biotinylated VnP-8-DN1 dimer-coated plates for 30 min, after which a pull-down assay was performed with streptavidin beads and the level of c-Fms was then measured via immunoblotting. The biotinylated VnP-8-DN1 dimer was found to bind to c-Fms (Fig. 16), indicating that the VnP-8-DN1 dimer interacted with c-Fms in BMMs.

**VnP-8-DN1 dimer inhibits RANK expression during M-CSF and RANKL-induced osteoclastogenesis**

RANK expression depends on M-CSF signaling via its receptor c-Fms [68, 70]. Given that the VnP-8-DN1 dimer suppressed M-CSF and RANKL-induced signaling in BMMs, this study sought to determine whether RANK expression was affected by the VnP-8-DN1 dimer during M-CSF and RANKL-induced osteoclastogenesis. In the presence of M-CSF (30 ng/ml) and RANK (100 ng/ml), the level of RANK was increased in a time-dependent manner when BMMs were treated with the VnP-8-DN1 monomer (Fig. 17). In contrast, the VnP-8-DN1 dimer inhibited RANK expression. The inhibitory effect of the VnP-8-DN1 dimer on osteoclast differentiation resulted from M-CSF signaling malfunction during RANK expression. This result is consistent with Fig. 6,

which illustrates that the activation of MAPKs by RANKL is inhibited by the VnP-8-DN1 dimer.

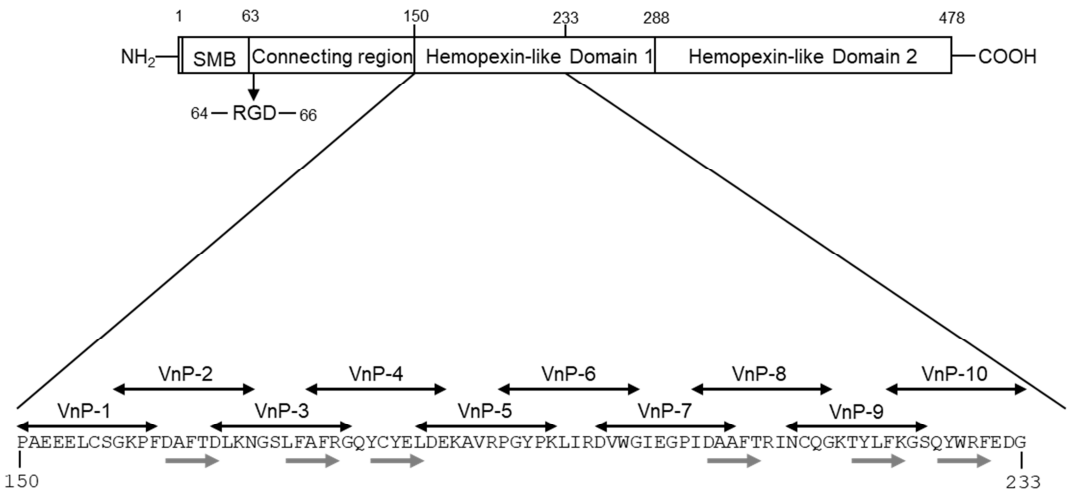


**Figure 1. The locations and amino acid sequences of the synthetic peptides derived from human vitronectin.** Each peptide (VnP-1 to VnP-10) consists of 12 amino acids corresponding to residues 150-233 of human vitronectin hemopexin-like domain 1. Locations of the synthetic peptides are represented by arrows.β-strands are indicated by the gray arrows.

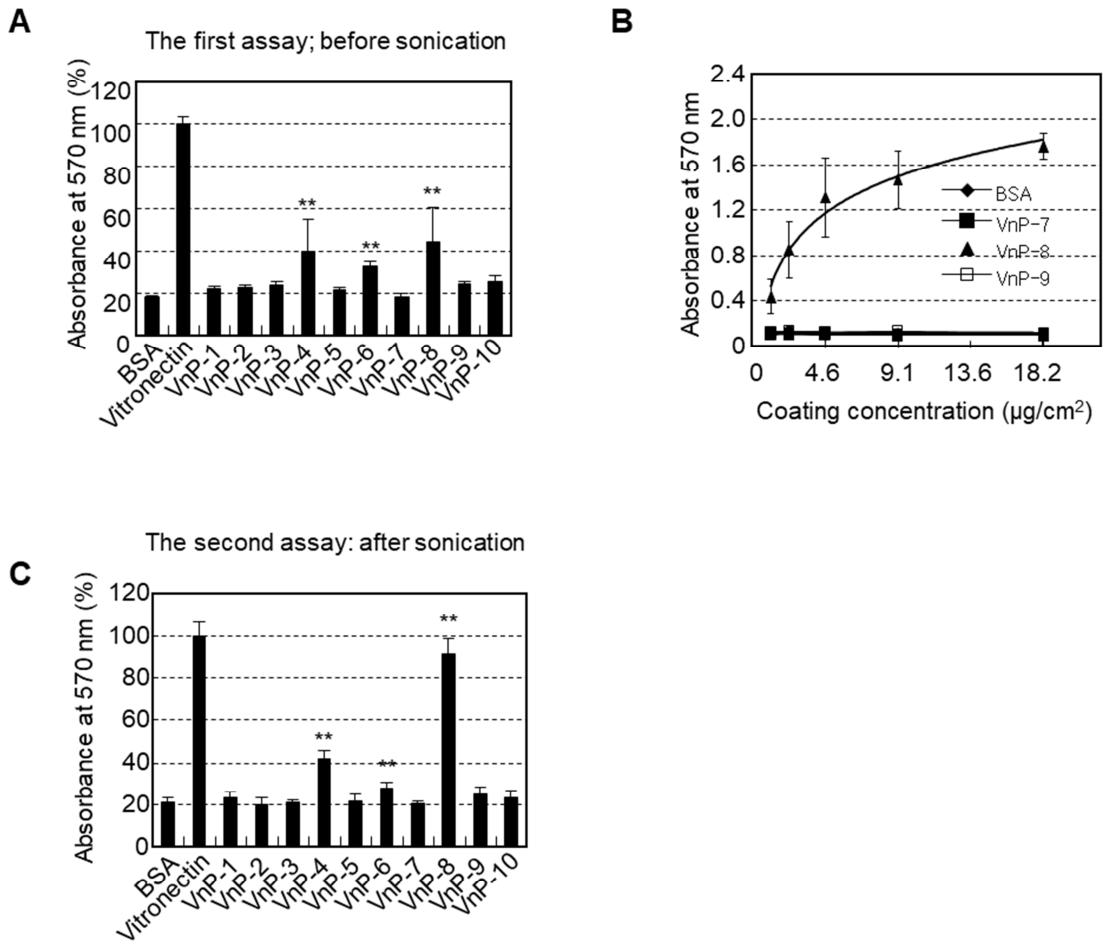


**Figure 2. Cell attachment of osteogenic cells to synthetic peptides.** (A) 48-well plates were coated with 9.1 μg/cm$^2$ synthetic peptides, 1% BSA or 0.23 μg/cm$^2$ vitronectin, and osteogenic cells were seeded and cultured for 1 h in serum-free medium. (B) Dose-dependent cell attachment of VnP-8. The plates were immobilized with various concentrations of peptides by air drying, and osteogenic cells were incubated to attach for 1 h in serum-free medium. (C) Peptides solution was sonicated for 10 sec 3 times, and then stored for 5 days at room temperature. Triplicate experiments gave similar results. Data are mean ± SD (n = 4). ** $P < 0.01$ versus BSA-coated group.

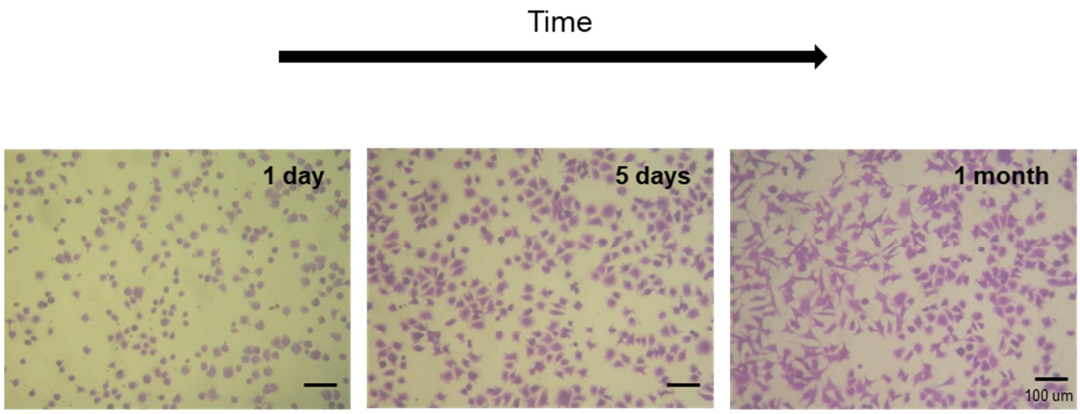


**Figure 3. Morphological changes of Hos cells to VnP-8-mediated attachment.** VnP-8 was stored at room temperature for 1 day, 5 days and 1 month. Then, in the culture dish coated with each peptide, cells were seeded onto peptide-coated plates and cultured for 3 h in serum-free medium. The fixed cells were stained with 0.5% crystal violet and photographed. Scale bar, 100 μm.

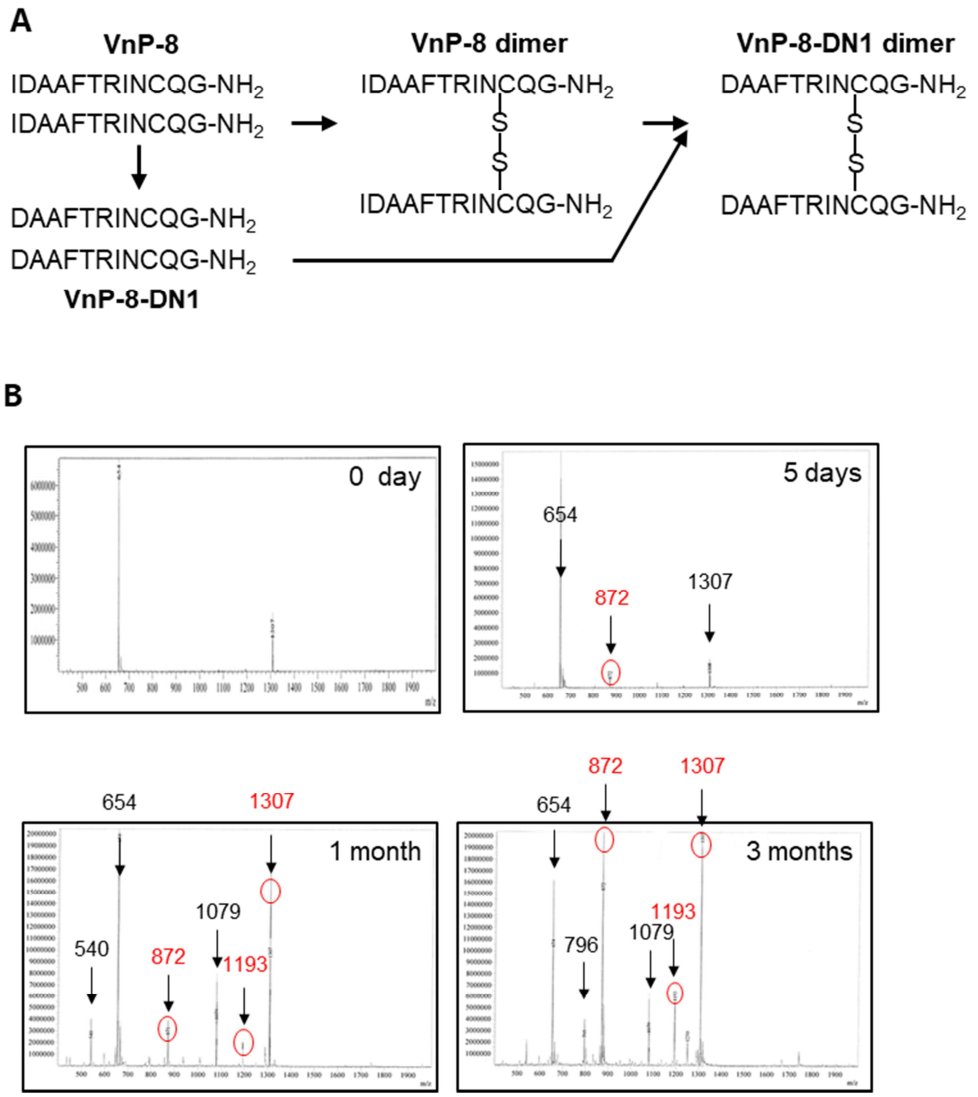


**Figure 4. Modification of the VnP-8 by spontaneous air oxidation.** VnP-8 stock solutions (5 mg/ml) were sonicated 10 sec for 3 times, and stored at room temperature for 5 days, 1 month or 3 months each. (A) Scheme of putative modification of amino acids in the VnP-8 sequence. (B) LC-MS profiles of modified peptides. The red ovals indicate the dimeric form of VnP-8 or VnP-8-DN1.

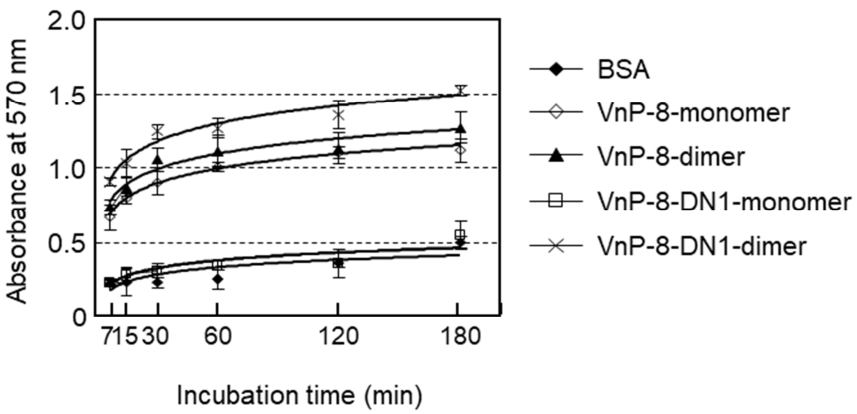


**Figure 5. Effects of cell attachment to modified VnP-8 peptides.** Cell attachment to peptide-coated plates in osteogenic cells over a time course. Cells were cultured for 7, 15, 30, 60, 120, and 180 min in serum-free medium. Data are mean ± SD (n = 4).

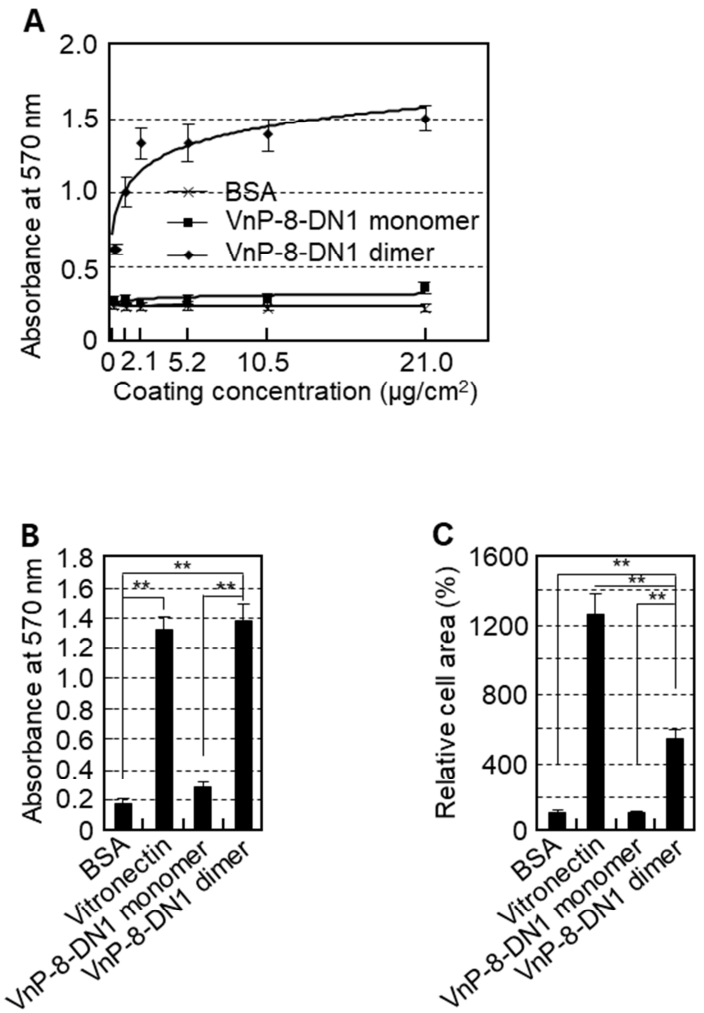


**Figure 6. VnP-8-DN1 dimer promotes cell attachment and spreading in osteogenic cells.** (A) Dose-dependent cell attachment of VnP-8-DN1 dimer. The plates were immobilized with various concentrations of peptides by air drying, and osteogenic cells were allowed to attach for 1 h in serum-free medium. (B) Attachment of osteogenic cells to VnP-8-DN1 dimer for 1 h and spreading for 3 h. (C) Data are mean ± SD (n = 4). ** $P < 0.01$.

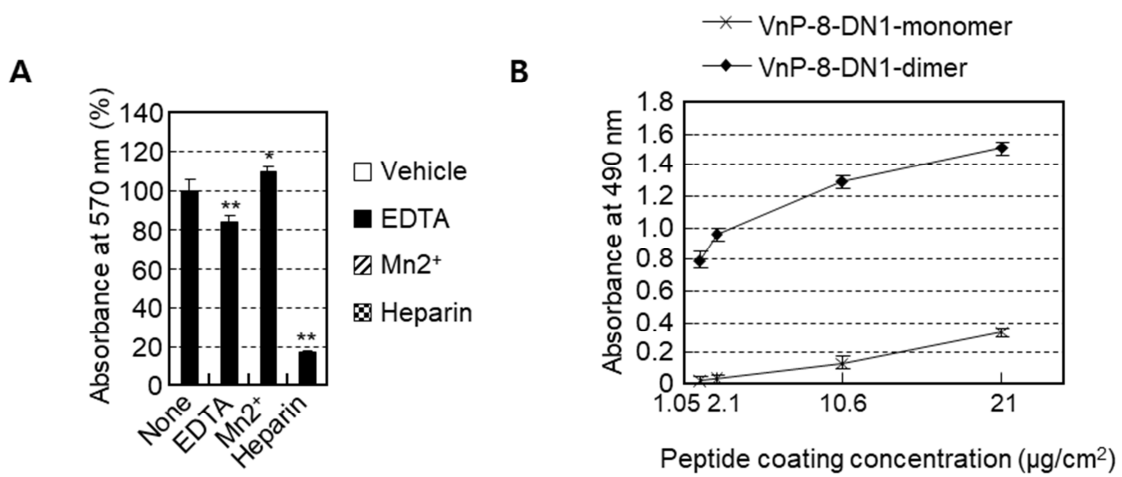


**Fig 7. Binding activity of heparin to the VnP-8-DN1 dimer.** (A) Inhibition of cell attachment to VnP-8-DN1 dimer by heparin. Cells were treated with 5mM EDTA, 500 μM $MnCl_2$, 100 μg/ml heparin for 10 min. The pretreated cells were allowed to attach for 1 h. (B) Synthetic peptides were coated onto enzyme-linked immunosorbent assay plates for 12 h at 4°C, subjected to blocking with 3% BSA for 2 h at 37°C, and then incubated with 10 ng/well of biotinylated heparin for 1 h at 37°C. The synthetic peptides bound biotin-conjugated heparin was captured using streptavidin-conjugated horseradish peroxidase. Data are mean ± SD (n = 4). ** $P < 0.01$, * $P < 0.05$ versus non-treated group.

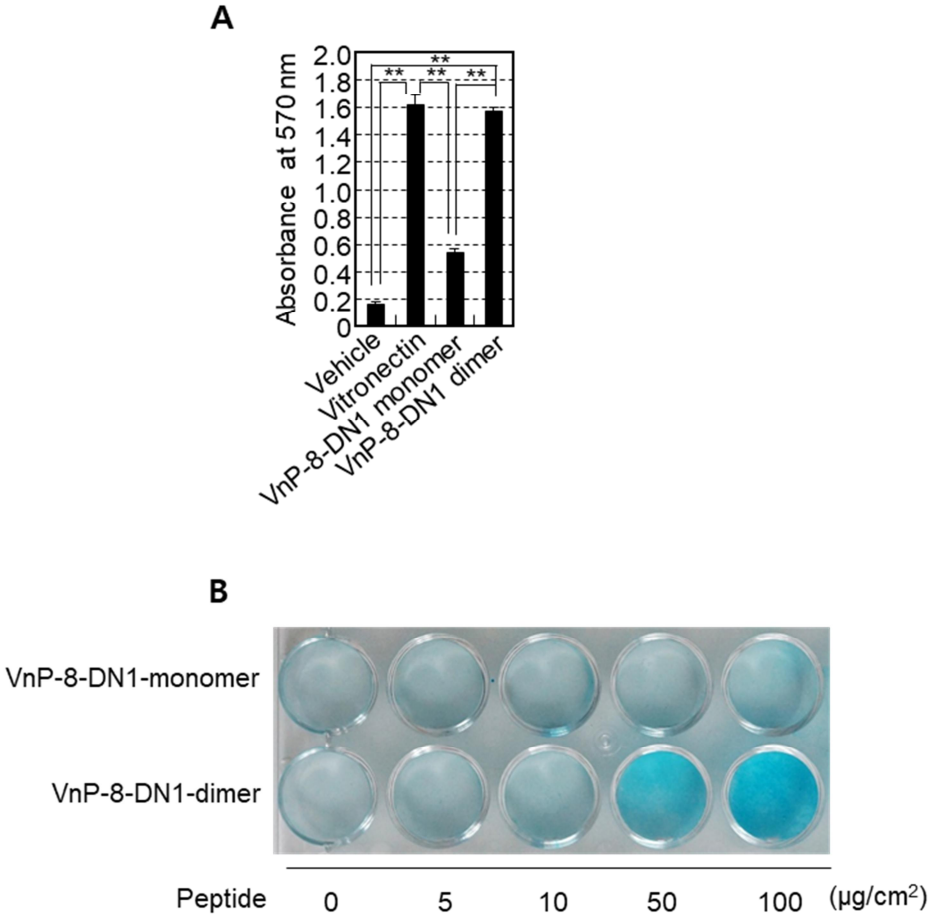
A
Absorbance at 570 nm
2.0
1.8
1.6
1.4
1.2
1.0
0.8
0.6
0.4
0.2
0
**
**
**
**
**
Vehicle
Vitronectin
VnP-8-DN1 monomer
VnP-8-DN1 dimer
B
VnP-8-DN1-monomer
VnP-8-DN1-dimer
Peptide
0
5
10
50
100
(μg/cm2)
C
Aggrecan
Fold increase in RAN
45
40
35
30
25
20
15
10
5
0
**
**
ITS
BMP-2
VnP-8-DN1-dimer
Col2α1
Fold increase in RAN
14
12
10
8
6
4
2
0
**
**
ITS
BMP-2
VnP-8-DN1-dimer

**Figure 8. Effects of the VnP-8-DN1 dimer on chondrogenic cell attachment and differentiation.** (A) Cells were seeded on peptide-coated plates and cultured for 1 h in serum-free medium. (B) Cells were cultured in growth medium containing peptides without 1X antibiotics+ 1X insulin-transferrin-sodium selenite (ITS)) for 14 days, and then stained with 0.1% Alcian blue. (C) Real-time PCR for chondrogenic markers, aggrecan and collagen type Ⅱ α1 (Col2α1). ATDC5 cells (8 x $10^4$ cells/24 well) were cultured in chondrogenic differentiation medium (DMEM/F12 + 5% FBS + 1X antibiotics+ 1X insulin-transferrin-sodium selenite (ITS) containing BMP (10 ng/ml) or VnP-8-DN1 dimer (100 μg/ml) for 7 days. Data are mean ± SD (n = 4). ** $P < 0.01$.

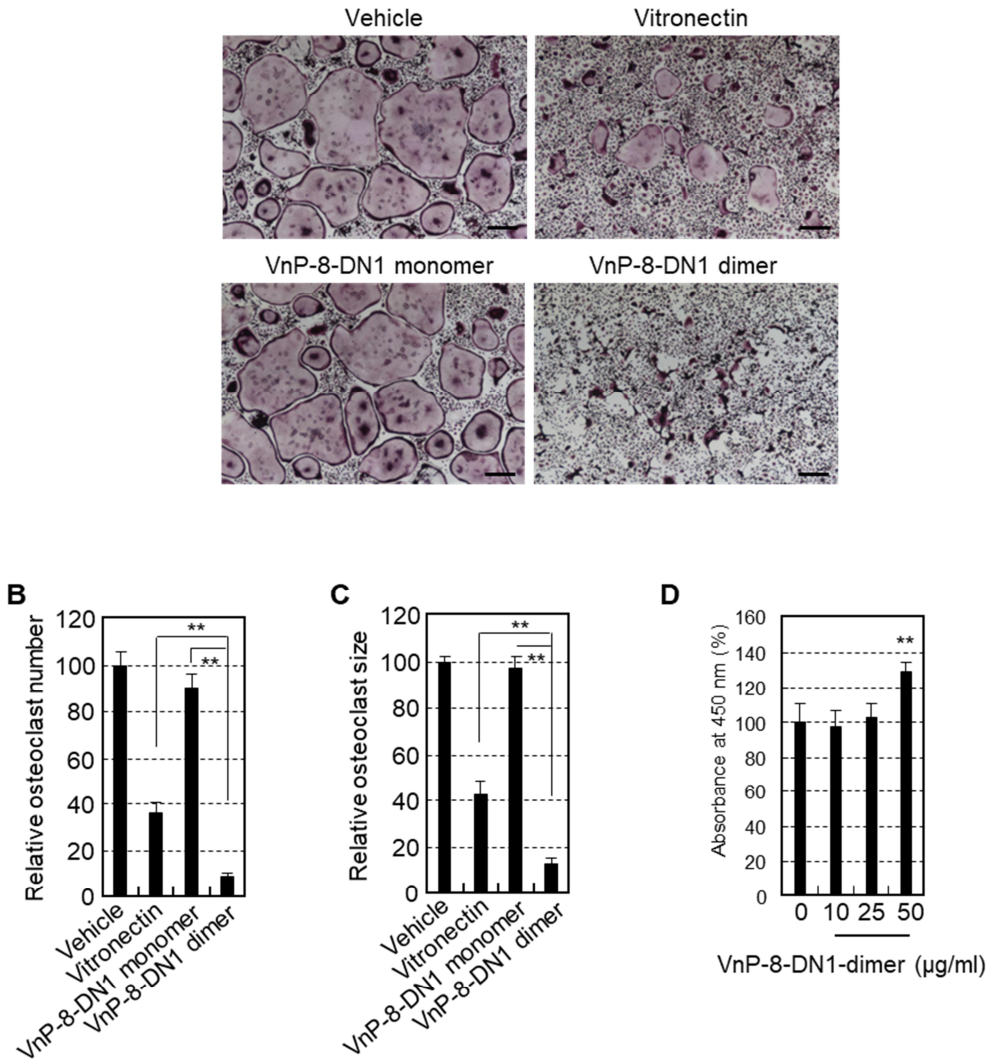


**Figure 9. The inhibitory effects of immobilized VnP-8-DN1 dimer on M-CSF and RANKL-induced osteoclast differentiation.** (A) BMMs were cultured for 4 days on VnP-8-DN1 monomer or dimer-coated culture dishes in the presence of 30 ng/ml M-CSF and 100 ng/ml RANKL. The differentiated cells were fixed and stained for TRAP. (B) TRAP-positive multinucleated cells with three or more nuclei were regarded as osteoclasts. (C) The sizes of the osteoclasts were imaged using a light microscopy and measured by the maximum diameters of multinucleated TRAP-positive cells. (D) Cell viability of osteogenic cells treated with VnP-8-DN1 dimer for 48 h. Scale bars, 200 μm. Data are mean ± SD (n = 4). ** $P < 0.01$. Scale bar, 500 μm.

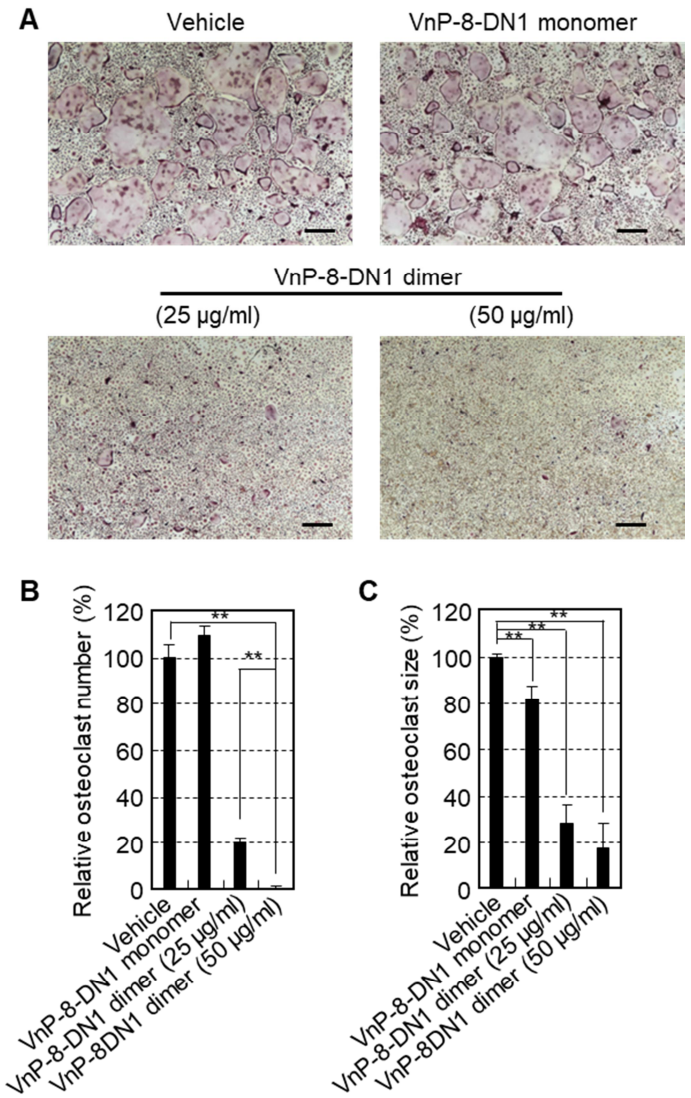


**Figure 10. The inhibitory effect of the VnP-8-DN1 dimer on M-CSF and RANKL-induced osteoclast differentiation.** (A) BMMs were cultured for 4 days in a medium containing VnP-8-DN1 monomer or dimer in the presence of 30 ng/ml M-CSF and 100 ng/ml RANKL. The differentiated cells were fixed and stained for TRAP. (B) TRAP-positive multinucleated cells with three or more nuclei were regarded as osteoclasts. (C) The sizes of the osteoclasts were imaged using a light microscopy and measured by the maximum diameters of multinucleated TRAP-positive cells. Data represent the means ± SD (n = 4). $^{**}P < 0.01$. Scale bar, 500 μm.

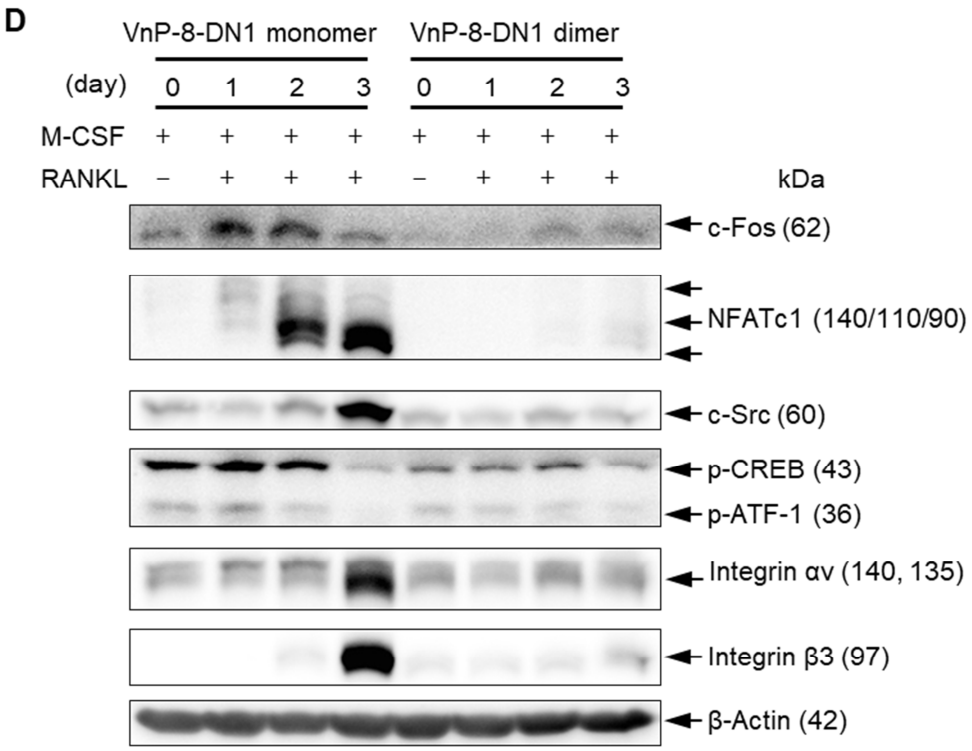


**Figure 11. Effect of the VnP-8-DN1 dimer on osteoclastogenic marker proteins expression in BMMs.** BMMs were cultured in the presence of 30 ng/ml M-CSF and 100 ng/ml RANKL and treated with VnP-8-DN1 dimer for the indicated times. Cell lysates were analyzed immunoblotting using specific antibodies for c-Fos, NFATc1, c-Src, p-CREB, Integrin αv, and Integrin β3. β-actin served as a loading control.

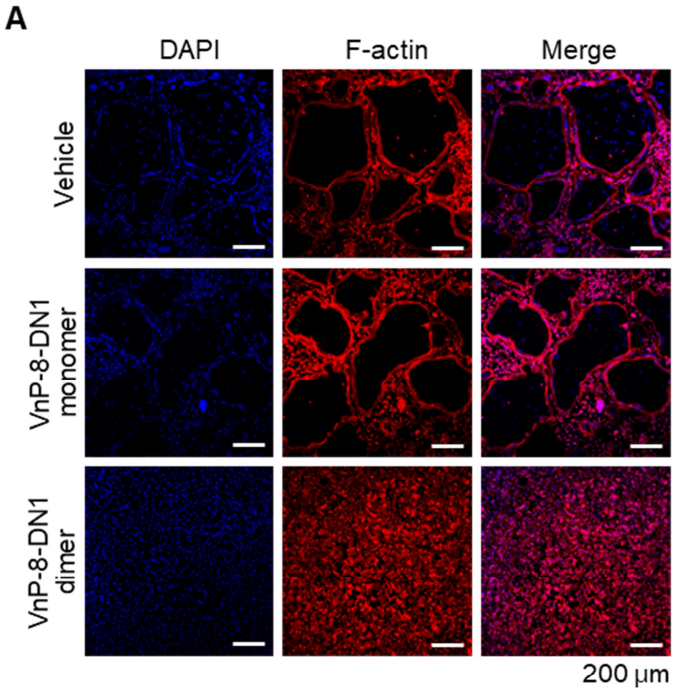
A
DAPI
F-actin
Merge
Vehicle
VnP-8-DN1 monomer
VnP-8-DN1 dimer
200 μm

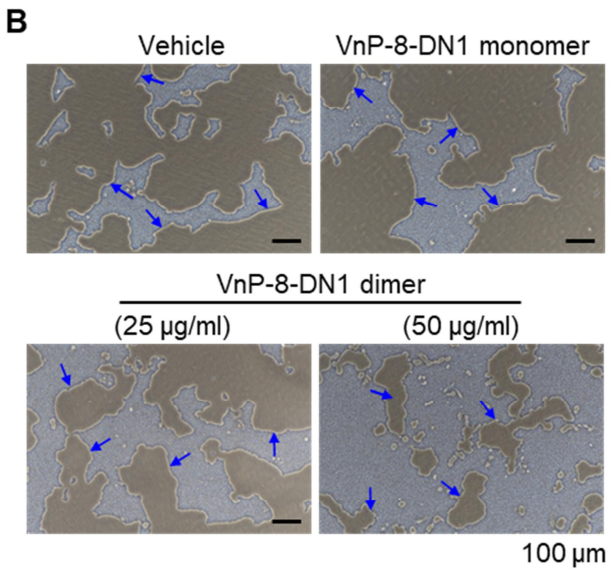
B
Vehicle
VnP-8-DN1 monomer
VnP-8-DN1 dimer
(25 μg/ml)
(50 μg/ml)
100 μm

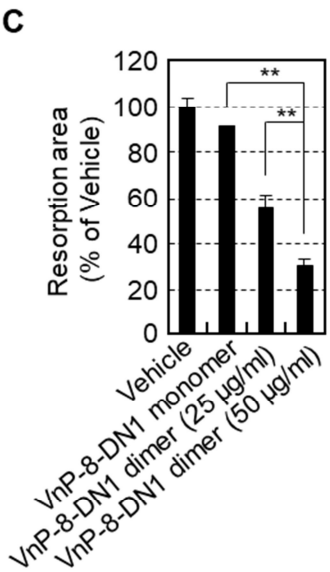
C
Resorption area
(% of Vehicle)
120
100
80
60
40
20
0
**
**
Vehicle
VnP-8-DN1 monomer
VnP-8-DN1 dimer (25 μg/ml)
VnP-8-DN1 dimer (50 μg/ml)

**Figure 12. Effect of the VnP-8-DN1 dimer on cytoskeletal organization and resorption function.** (A) BMMs were cultured in the presence of M-CSF (30 ng/ml) and RANKL (100 ng/ml) for 4 days with VnP-8-DN1 monomer or dimer. The cells were was stained with DAPI (blue) for nuclei and rhodamine-phalloidin for F-actin (red). (B) BMMs were plated on calcium-coated osteo assay plate in the differentiation medium with or without VnP-8-DN1 dimer for 4 days. Osteoclasts were removed with 10% Clorox (0.56% NaOCl). The resorption area was imaged and (C) analyzed with Image-Pro Plus 4.5 program (Media cybernetics). Data represent mean ± SD. $^{**}P < 0.01$. Scale bar, 100 μm.

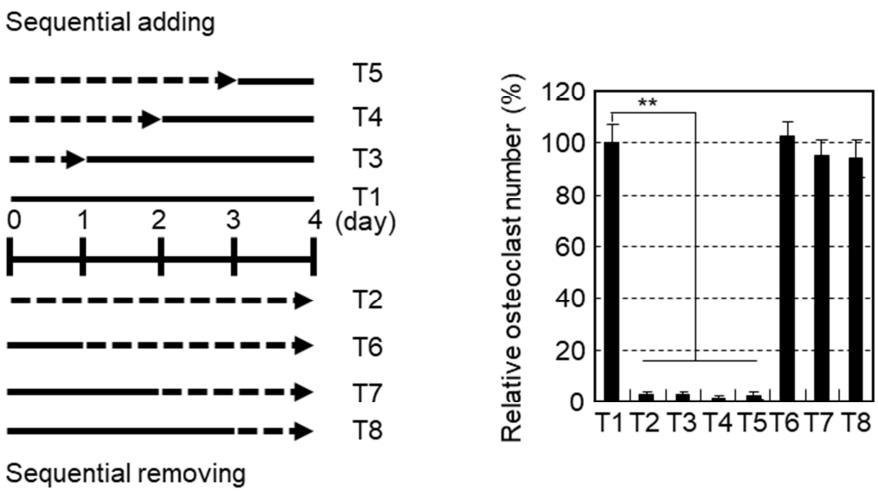


**Figure 13. VnP-8-DN1 dimer inhibits osteoclastogenesis in the early differentiation stage.** BMMs were cultured for 4 days in the presence of 30 ng/ml M-CSF and 100 ng/ml RANKL and treated with VnP-8-DN1 dimer (50 μg/ml) for the indicated times; For the first 1 day (T3), the first 2 days (T4), the first 3 days (T5), all 4 days (T2), the last 1 day (T8), the last 2 days (T7), the last 3 days (T6), and vehicle (T1), Data represent mean ± S.D. $^{**}P < 0.01$ versus non-treated group.

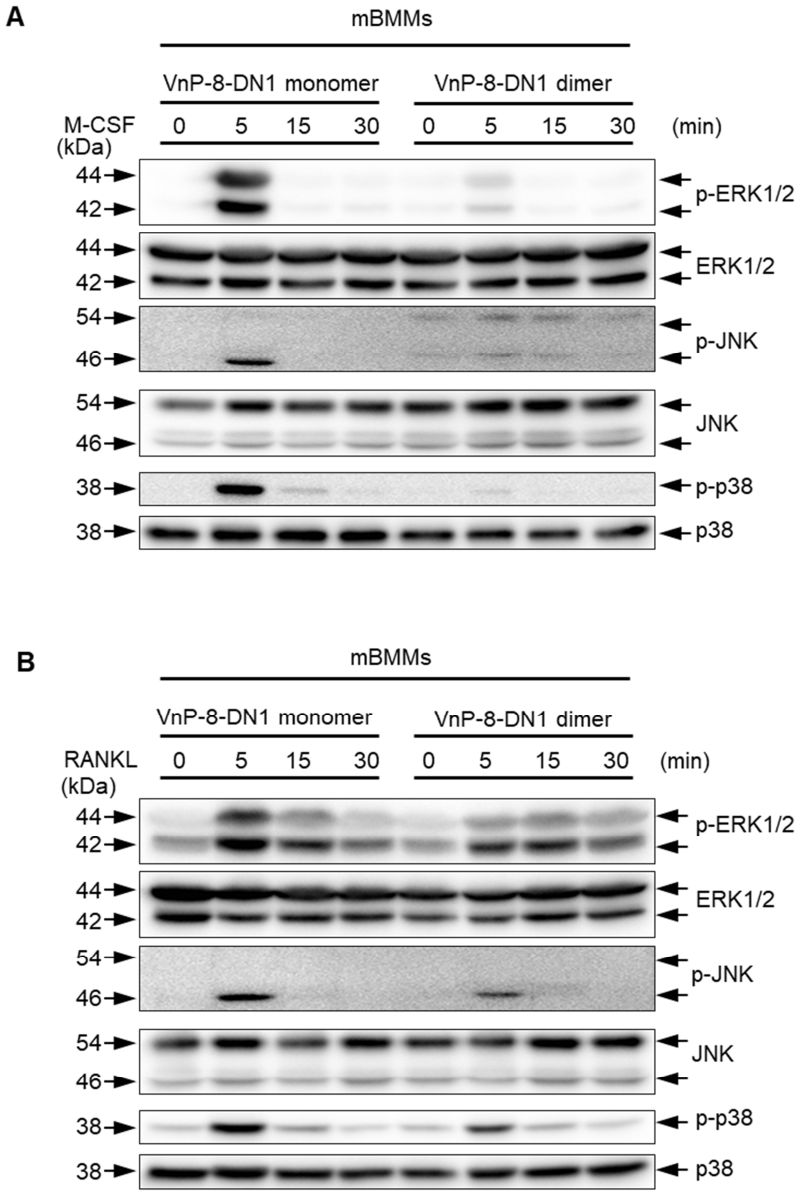


**Figure 14. Effects of the VnP-8-DN1 dimer on M-CSF or RANKL-stimulated signaling.** BMMs were cultured for 1 day in the presence of each peptide, serum-starved for 2 h, and pretreated with peptides (50 μg/ml) for 1 h. The preincubated cells were stimulated with 30 ng/ml M-CSF (A) or 100 ng/ml RANKL (B) for indicated times. Cell lysates were subjected to immunoblotted.

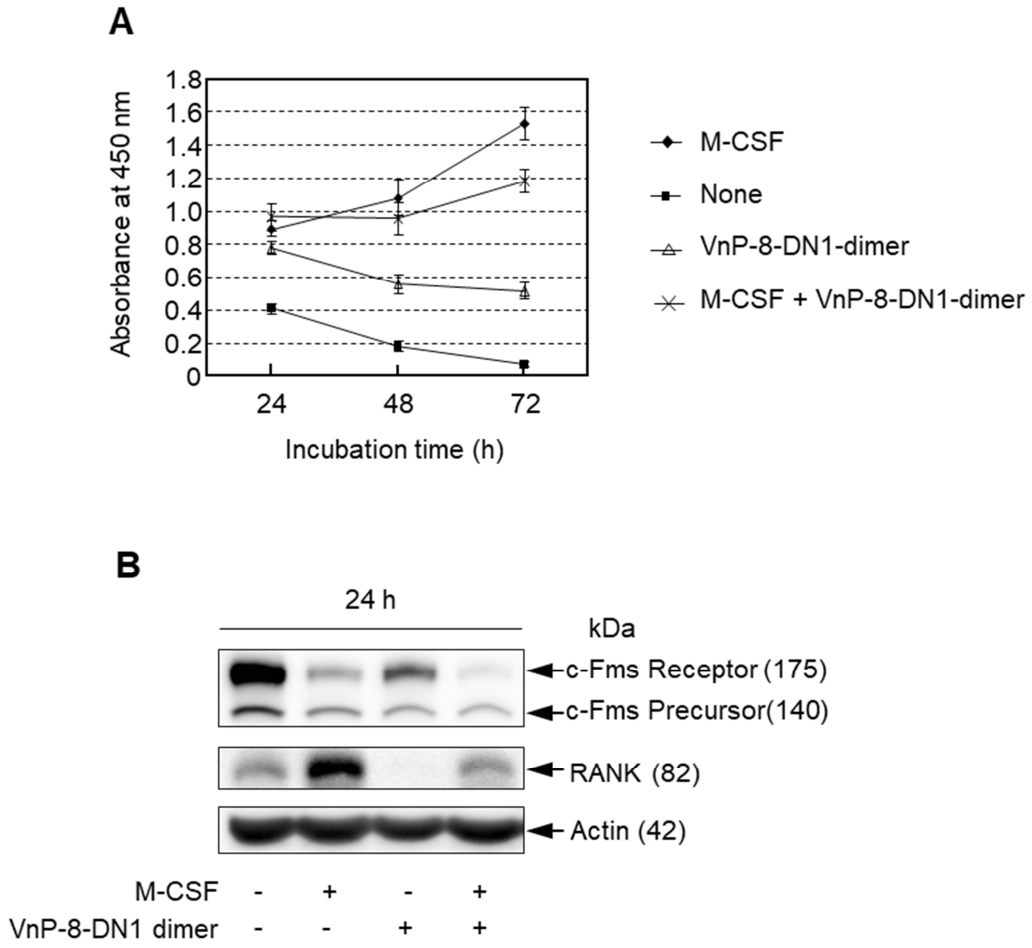


**Figure 15. The effect of the VnP-8-DN1 dimer on cell viability and c-Fms level in BMMs.** BMMs were cultured with M-CSF (30 ng/ml), peptide (50 μg/ml), and both M-CSF (30 ng/ml) and VnP-8-DN1 dimer (50 μg/ml) for 24, 48, and 72 h. None indicates medium alone. (A) Cell viability was measured by WST assay. Data represent mean ± S.D. $^{**}P < 0.01$. (B) The cells conditions in the assay were the same as described in (A), except that cells were cultured for 24 h. c-Fms and RANK levels by immunoblot analysis. β-actin served as a loading control.

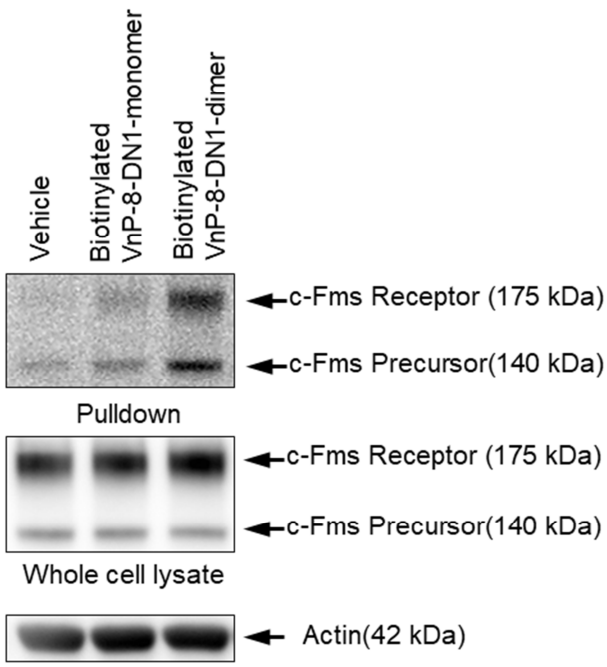


**Figure 16. VnP-8-DN1 dimer interacts with c-Fms.** BMMs were cultured for 2 h with vehicle, biotin-conjugated peptides (50 μg/ml). The association of VnP-8-DN1 dimer with c-Fms was captured by pull–down assay using streptavidin agarose beads. Cell lysates were subjected to immunoblot analyses.

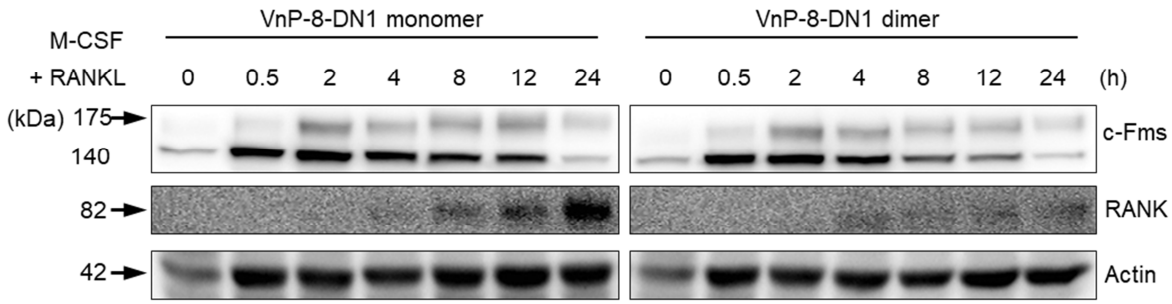


**Figure 17. Reduction of RANK expression by VnP-8-DN1 dimer.** BMMs were cultured for indicated times in the presence of M-CSF and RANKL with VnP-8-DN1 monomer or dimer (50 μg/ml). Expression levels of c-Fms and RANK were determined by immunoblot.

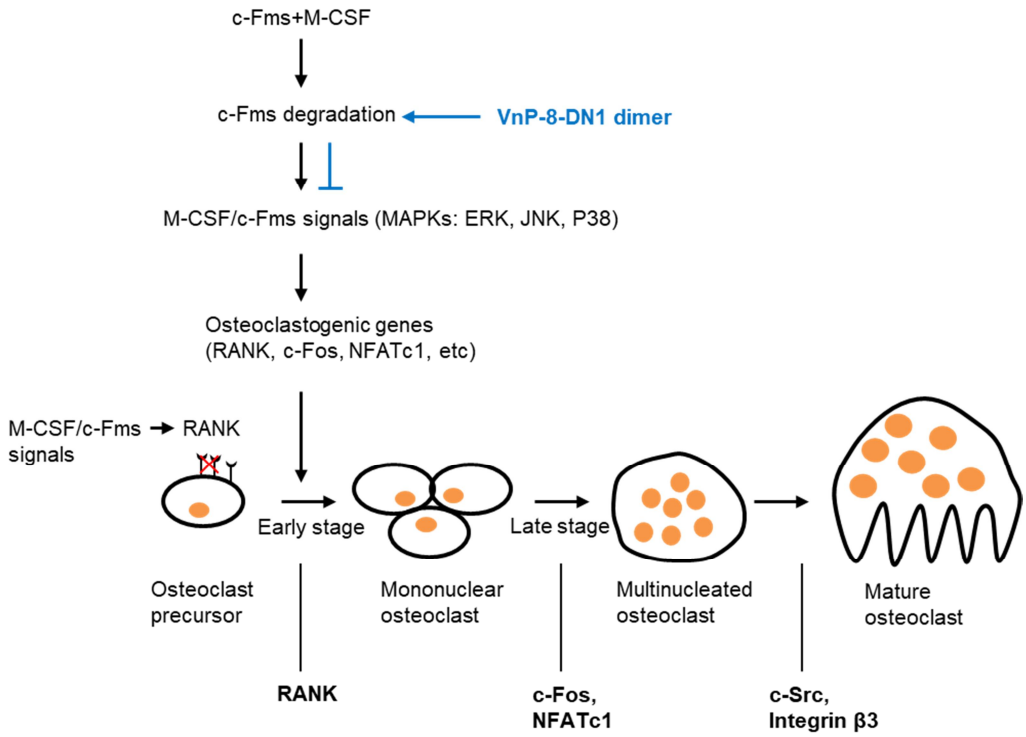


**Figure 18. Proposed pathways for inhibitory effect by the association of c-Fms with VnP-8-DN1 dimer on osteoclast differentiation.**

# DISCUSSION

There have been many studies to mimic the active site of proteins in tissue regeneration and treatment of diseases [2,4,7]. In this study, a bioactive peptide was screened via a cell attachment assay in osteogenic cells, and a cell-binding sequence (i.e., the IDAAFTRINCQG motif) was identified within human vitronectin. The peptide was then converted into a more stable and bioactive VnP-8-DN1 dimer through an air oxidation reaction. The VnP-8-DN1 dimer promoted ATDC5 cell attachment and chondrocyte differentiation and suppressed osteoclast differentiation.

Given that VnP-8 could not be easily dissolved in DDW, consistent cell attachment assay results could not be obtained. Vigorous vortexing and heat treatment of the peptide did not work well, but it was possible to develop an improved dimeric peptide through sonication and spontaneous air oxidation. Peptide solution sonication is routinely used to facilitate and accelerate the dissolution of macromolecules in both aqueous and organic solvents. Sonication-facilitated VnP-8 solubility enhancement induced natural oxidation of cysteine residues to form dimers, which in turn increased cell attachment. Several reports showed that peptide dimerization induces functional enhancement. The dimeric formation of short synthetic cationic peptides resulted in a 60-fold enhancement in antimicrobial activity [72,73]. Furthermore, dimerization of antimicrobial peptides in conjunction with backbone cyclization improved both the potency and stability of linear peptides [74]; however, the underlying mechanisms of these phenomena remain unclear. In general, to increase the proteolytic stability of bioactive peptides in *vivo*, the peptide

was modified and designed and synthesized by arbitrary inclusion of double (or single) cysteine residues in its structure [75]. However, additional research is needed to determine the differences between VnP-8-DN1 monomer and dimer activities. Moreover, further studies are also needed to identify VnP-8-DN1 dimer cell surface receptors through structural binding site analysis.

In general, a strong heparin-binding affinity can predict the potential of a protein to bind matrix- or membrane-bound heparan sulfate proteoglycans. Lysine-arginine-serine-arginine (KRSR), a putative heparin-binding site commonly found in bone sialoprotein, vitronectin, fibronectin, osteopontin, and thrombospondin, could enhance attachment activity of osteoblasts and expression of the osteogenic gene. [76,77]. The phenylalanine-histidine-arginine-arginine-isoleucine-lysine-alanine (FHRRIKA), a heparin-binding sequence of bone sialoprotein, improved the ability of osteoblast attachment, spreading and bone matrix mineralization [78,79]. VnP-8 increased the cell attachment activity in osteogenic cells and chondrocyte precursors, as well as differentiated chondrocyte precursors into chondrocytes, and it is thought that heparin-binding activity plays an important role in these effects.

In the early stages of tissue regeneration, peptides must elicit cell responses as much as possible through the attachment of tissue cells. Cellular responses can be maximized by using other active peptides in combination. Syndecan□ and integrin□binding peptides have been demonstrated to synergistically promoted cell attachment [80]. The VnP-8-DN1 dimer showed a strong cell attachment capacity via heparin-binding activity, induced chondrogenic differentiation, and inhibited osteoclast formation. Importantly, this peptide could be further developed into an effective therapeutic agent through the

addition and modification of its functional groups or by increasing the adsorption rate of the peptide to the biomaterial implanted in the tissue. Therefore, the VnP-8-DN1 dimer may become a useful bone regeneration agent through additional research, including the identification of its mechanisms of action.

Osteoclast formation consists of the multi-step phase comprising the proliferation and recruitment of osteoclast precursors, commitment to osteoclast precursors, fusion into multinucleated cells, and maturation of multinucleated osteoclast [20]. At the early stage of osteoclastogenesis, signaling of the M-CSF/c-Fms axis contributes to cell survival, proliferation, and differentiation of osteoclast precursors [41]. The VnP-8-DN1 dimer inhibited the differentiation of BMMs into osteoclasts at an early stage during osteoclastogenesis. Furthermore, not only the expression of induction of NFATc1 itself but also, NFATc1-dependent and -independent osteoclast differentiation markers, were suppressed by the VnP-8-DN1 dimer. Moreover, even if the VnP-8-DN1 dimer was administered on the first trial day and then removed during the rest of the trial period, osteoclast differentiation capacity was not recovered. These results support the notion that the VnP-8-DN1 dimer inhibited osteoclast formation by targeting an early stage of osteoclastogenesis.

Peptides can be used to block key signaling pathways associated with osteoclast differentiation or function. Treatment strategies to overcome osteoclast hyperactivation can be established by inducing osteoclast apoptosis, inhibiting osteoclast differentiation, and impairing bone resorption. Among these, the VnP-8-DN1 dimer acted at the initial stage by association with c-Fms during osteoclastogenesis and inhibited osteoclast precursor differentiation into osteoclasts. Previous reports demonstrate that M-CSF plays

a critical role not only in osteoclast precursor proliferation but also in the regulation of the resorption activity of mature osteoclast [81]. Although the effect of promoting osteoclast differentiation is apparent, there are contradictory results on the effect of regulating the absorption activity of mature osteoclasts [82]. Therefore, further studies are needed to characterize the effects of the VnP-8-DN1 dimer, which interacts with c-Fms, on the bone resorption of mature osteoclast.

Similar to other receptor-ligand interactions, binding of M-CSF to c-Fms leads to internalization and degradation of c-Fms in the lysosome [83]. BMMs maintain a high c-Fms level on their surface in the absence of M-CSF. However, the level of cell surface c-Fms decreased when the BMMs were treated with the VnP-8-DN1 dimer. The mechanisms by which the VnP-8-DN1 dimer inhibits osteoclast differentiation was the inhibition of M-CSF signaling that is required for RANK expression, which was mediated by downregulation of cell surface c-Fms expression. This mechanism is similar to that of osteoclast differentiation inhibition via Toll-like receptors (TLRs) in human osteoclast precursors. TLR stimulation of human osteoclast precursors strongly inhibits their differentiation into multinucleated, mature osteoclasts induced by TNF-related activation-induced cytokine, and also targets c-Fms and inhibits M-CSF-induced RANK expression [84]. However, inhibition via TLRs does not affect the expression of c-Fms in mouse osteoclasts [85,86]. Therefore, our study concluded that the VnP-8-DN1 dimer interacted mainly with c-Fms, and not as a ligand of TLRs.

Improper handling and storage of peptide lead to modification and degradation of peptides, which can affect the function of the peptides. Therefore, whenever possible, peptides should be maintained in lyophilized form prior to analysis, and peptide solutions

should be stored away from light at -20 °C [87,88]. Particularly, peptides containing cysteine, tryptophan, or methionine can be readily oxidized and result in the generation of modified peptides, such as peptides with oxidized side chain groups, peptide fragments resulting from backbone damage, and dimerized or aggregated peptides [59,89]. These modifications can cause a decrease in the activity of the peptide or even a complete loss of activity. Moreover, decreased peptide activity over time may result in insufficient analytical reproducibility and increased experimental data variability. However, the VnP-8 peptide identified in this study exhibited an interesting phenomenon by which its activity was rather enhanced by oxidation.

In this study, the VnP-8-DN1 dimer suppressed osteoclast differentiation at the early stage of osteoclastogenesis through interaction with c-Fms, thereby downregulating M-CSF and RANKL-induced activation of MAPKs and RANK expression (Fig. 18). Taken together, these results suggest that the VnP-8-DN1 dimer is a promising new anti-resorptive agent to suppress bone resorption by inhibiting osteoclast differentiation.

# CONCLUSION

In this study, an IDAAFTRINCQG motif was identified within the human vitronectin hemopexin-1 region and was found to promote cell attachment in osteogenic cells. Additionally, an isoleucine residue was removed from the N-terminus of the VnP-8 peptide, resulting in the formation of a disulfide bond between two cysteine residues to form the dimeric peptide VnP-8-DN1 dimer. The VnP-8-DN1 dimer induced chondrogenic differentiation of ATDC5 cells and inhibited osteoclast differentiation in BMMs. The VnP-8-DN1 dimer inhibited osteoclast differentiation by associating with the M-CSF receptor c-Fms in the early stages of osteoclast formation, thereby inhibiting the activation of MAPKs induced by M-CSF and RANKL. This, in turn, reduced RANK expression, thereby inhibiting osteoclast differentiation. These results suggest that the VnP-8-DN1 dimer might be a promising therapeutic agent for osteoclast-mediated bone disease and bone regeneration.

# REFERENCES


1. Langer R, Vacanti JP. Tissue engineering. Science. 1993;260:920-6.
2. Cai L, Heilshorn SC. Designing ECM-mimetic materials using protein engineering. Acta Biomater. 2014;10:1751-60.
3. Hutmacher DW. Scaffolds in tissue engineering bone and cartilage. Biomaterials. 2000;21:2529-43.
4. Chan BP, Leong KW. Scaffolding in tissue engineering: general approaches and tissue-specific considerations. Eur Spine J. 2008;17:S467-S79.
5. Hynes RO, Zhao Q. The evolution of cell adhesion. J Cell Biol. 2000;150: 89-96.
6. Zhang HN, Hollister S. Comparison of Bone Marrow Stromal Cell Behaviors on Poly(caprolactone) with or without Surface Modification: Studies on Cell Adhesion, Survival and Proliferation. J Biomat Sci-Polym E. 2009;20:1975-93.
7. Wang CY, Liu Y, Fan YB, Li XM. The use of bioactive peptides to modify materials for bone tissue repair. Regen Biomater. 2017;4:191-206.
8. Agrawal CM, Ray RB. Biodegradable polymeric scaffolds for musculoskeletal tissue engineering. J Biomed Mater Res. 2001;55:141-50.
9. Ohara H, Ichikawa S, Matsumoto H, Akiyama M, Fujimoto N, Kobayashi T, et al. Collagen-derived dipeptide, proline-hydroxyproline, stimulates cell proliferation and hyaluronic acid synthesis in cultured human dermal fibroblasts. J Dermatol. 2010;37:330-8.
10. Danen EH, Aota S, van Kraats AA, Yamada KM, Ruiter DJ, van Muijen GN.

Requirement for the synergy site for cell adhesion to fibronectin depends on the activation state of integrin alpha 5 beta 1. J Biol Chem. 1995;270:21612-8.

11. Hibino S, Shibuya M, Engbring JA, Mochizuki M, Nomizu M, Kleinman HK. Identification of an active site on the laminin alpha 5 chain globular domain that binds to CD44 and inhibits malignancy. Cancer Res. 2004;64:4810-6.
12. Jung SY, Kim JM, Min SK, Kim OB, Jang DH, Kang HK, et al. The potential of laminin-2-biomimetic short peptide to promote cell adhesion, spreading and migration by inducing membrane recruitment and phosphorylation of PKC delta. Biomaterials. 2012;33:3967-79.
13. Bellis SL. Advantages of RGD peptides for directing cell association with biomaterials. Biomaterials. 2011;32:4205-10.
14. Li ZH, Cao B, Wang X, Ye K, Li SY, Ding JD. Effects of RGD nanospacing on chondrogenic differentiation of mesenchymal stem cells. J Mater Chem B. 2015;3:5197-209.
15. Yeo IS, Min SK, Kang HK, Kwon TK, Jung SY, Min BM. Identification of a bioactive core sequence from human laminin and its applicability to tissue engineering. Biomaterials. 2015;73:96-109.
16. Choi YJ, Lee JY, Park JH, Park JB, Suh JS, Choi YS, et al. The identification of a heparin binding domain peptide from bone morphogenetic protein-4 and its role on osteogenesis. Biomaterials. 2010;31:7226-38.
17. Min SK, Kang HK, Jung SY, Jang DH, Min BM. A vitronectin-derived peptide reverses ovariectomy-induced bone loss via regulation of osteoblast and osteoclast differentiation. Cell Death Differ. 2018;25:268-81.

18. Bonucci E. The organic-inorganic relationships in bone matrix undergoing osteoclastic resorption. Calcif Tissue Res. 1974;16:13-36.
19. Tanaka S, Takahashi N, Udagawa N, Tamura T, Akatsu T, Stanley ER, et al. Macrophage Colony-Stimulating Factor Is Indispensable for Both Proliferation and Differentiation of Osteoclast Progenitors. J Clin Invest. 1993;91:257-63.
20. Teitelbaum SL. Bone resorption by osteoclasts. Science. 2000;289(5484):1504-8.
21. Wiktorjedrzejczak W, Bartocci A, Ferrante AW, Ahmedansari A, Sell KW, Pollard JW, et al. Total Absence of Colony-Stimulating Factor 1 in the Macrophage-Deficient Osteopetrotic (Op Op) Mouse. P Natl Acad Sci USA. 1990;87:4828-32.
22. Kim N, Odgren PR, Kim DK, Marks SC, Choi YW. Diverse roles of the tumor necrosis factor family member TRANCE in skeletal physiology revealed by TRANCE deficiency and partial rescue by a lymphocyte-expressed TRANCE transgene. P Natl Acad Sci USA. 2000;97:10905-10.
23. Boyle WJ, Simonet WS, Lacey DL. Osteoclast differentiation and activation. Nature. 2003;423:337-42.
24. Feng X, McDonald JM. Disorders of Bone Remodeling. Annu Rev Pathol-Mech. 2011;6:121-45.
25. Hardy R, Cooper MS. Bone loss in inflammatory disorders. J Endocrinol. 2009;201:309-20.
26. Roodman GD. Osteoclast function in Paget's disease and multiple myeloma. Bone. 1995;17(2 Suppl):57S-61S.
27. Rodan GA, Martin TJ. Therapeutic approaches to bone diseases. Science.

2000;289:1508-14.

28. Lee JY, Choi YS, Lee SJ, Chung CP, Park YJ. Bioactive Peptide-modified Biomaterials for Bone Regeneration. Curr Pharm Design. 2011;17:2663-76.
29. Fosgerau K, Hoffmann T. Peptide therapeutics: current status and future directions. Drug Discov Today. 2015;20:122-8.
30. Bi HD, Chen X, Gao S, Yu XL, Xiao J, Zhang B, et al. Key Triggers of Osteoclast-Related Diseases and Available Strategies for Targeted Therapies: A Review. Front Med-Lausanne. 2017;4:234.
31. Aoki K, Saito H, Itzstein C, Ishiguro M, Shibata T, Blanque R, et al. A TNF receptor loop peptide mimic blocks RANK ligand-induced signaling, bone resorption, and bone loss. J Clin Invest. 2006;116(6):1525-34.
32. Kim H, Choi HK, Shin JH, Kim KH, Huh JY, Lee SA, et al. Selective inhibition of RANK blocks osteoclast maturation and function and prevents bone loss in mice. J Clin Invest. 2009;119:813-25.
33. O'Brien FJ. Biomaterials & scaffolds for tissue engineering. Mater Today. 2011;14:88-95.
34. Klimek K, Ginalska G. Proteins and Peptides as Important Modifiers of the Polymer Scaffolds for Tissue Engineering Applications-A Review. Polymers (Basel). 2020;12:844.
35. Liggett W, Jr., Shevde N, Anklesaria P, Sohoni S, Greenberger J, Glowacki J. Effects of macrophage colony stimulating factor and granulocyte-macrophage colony stimulating factor on osteoclastic differentiation of hematopoietic progenitor cells. Stem Cells. 1993;11:398-411.

36. Lee KB, Johnson JS, Song KJ, Taghavi CE, Wang JC. Use of Autogenous Bone Graft Compared With RhBMP in High-risk Patients A Comparison of Fusion Rates and Time to Fusion. J Spinal Disord Tech. 2013;26:233-8.
37. Subbiah V, Madsen VS, Raymond AK, Benjamin RS, Ludwig JA. Of mice and men: divergent risks of teriparatide-induced osteosarcoma. Osteoporosis Int. 2010;21:1041-5.
38. Baker MP, Reynolds HM, Lumicisi B, Bryson CJ. Immunogenicity of protein therapeutics: The key causes, consequences and challenges. Self Nonself. 2010;1:314-22.
39. Raggatt LJ, Partridge NC. Cellular and Molecular Mechanisms of Bone Remodeling. Journal of Biological Chemistry. 2010;285:25103-8.
40. Paniagua RT, Chang A, Mariano MM, Stein EA, Wang Q, Lindstrom TM, et al. c-Fms-mediated differentiation and priming of monocyte lineage cells play a central role in autoimmune arthritis. Arthritis Res Ther. 2010;12:R32.
41. Ross FP. M-CSF, c-Fms, and signaling in osteoclasts and their precursors. Ann Ny Acad Sci. 2006;1068:110-6.
42. Lee K, Chung YH, Ahn H, Kim H, Rho J, Jeong D. Selective Regulation of MAPK Signaling Mediates RANKL-dependent Osteoclast Differentiation. Int J Biol Sci. 2016;12:235-45.
43. Takayanagi H, Kim S, Koga T, Nishina H, Isshiki M, Yoshida H, et al. Induction and activation of the transcription factor NFATc1 (NFAT2) integrate RANKL signaling in terminal differentiation of osteoclasts. Dev Cell. 2002;3:889-901.
44. Carron CP, Meyer DM, Engleman VW, Rico JG, Ruminski PG, Ornberg RL, et

al. Peptidomimetic antagonists of alpha v beta 3 inhibit bone resorption by inhibiting osteoclast bone resorptive activity, not osteoclast adhesion to bone. J Endocrinol. 2000;165:587-98.

45. Lark MW, Stroup GB, Hwang SM, James IE, Rieman DJ, Drake FH, et al. Design and characterization of orally active Arg-Gly-Asp peptidomimetic vitronectin receptor antagonist SB 265123 for prevention of bone loss in osteoporosis. J Pharmacol Exp Ther. 1999;291:612-7.
46. Preissner KT. Structure and Biological Role of Vitronectin. Annu Rev Cell Biol. 1991;7:275-310.
47. Schvartz I, Seger D, Shaltiel S. Vitronectin. Int J Biochem Cell Biol. 1999;31:539-44.
48. Seiffert D. Detection of vitronectin in mineralized bone matrix. J Histochem Cytochem. 1996;44:275-80.
49. Piccard H, Van den Steen PE, Opdenakker G. Hemopexin domains as multifunctional liganding modules in matrix metal loproteinases and other proteins. J Leukocyte Biol. 2007;81:870-92.
50. Stanley KK. Homology with hemopexin suggests a possible scavenging function for S-protein/vitronectin. FEBS Lett. 1986;199:249-53.
51. Maile LA, Busby WH, Sitko K, Capps BE, Sergent T, Badley-Clarke J, et al. The heparin binding domain of vitronectin is the region that is required to enhance insulin-like growth factor-I signaling. Mol Endocrinol. 2006;20:881-92.
52. Wilkins-Port CE, Sanderson RD, Tominna-Sebald E, McKeown-Longo PJ. Vitronectin's basic domain is a syndecan ligand which functions in trans to

regulate vitronectin turnover. Cell Commun Adhes. 2003;10:85-103.

53. Skubitz APN, Mccarthy JB, Qi Z, Yi XY, Furcht LT. Definition of a Sequence, Ryvvlpr, within Laminin Peptide F9 That Mediates Metastatic Fibrosarcoma Cell-Adhesion and Spreading. Cancer Res. 1990;50:7612-22.
54. Nomizu M, Yokoyama F, Suzuki N, Okazaki I, Nishi N, Ponce ML, et al. Identification of homologous biologically active sites on the N-terminal domain of laminin alpha chains. Biochemistry-Us. 2001;40:15310-7.
55. Livak KJ, Schmittgen TD. Analysis of relative gene expression data using real-time quantitative PCR and the $2^{-\Delta\Delta C}{}_{T}$ method. methods. 2001;25:402-8.
56. Maryas J, Faktor J, Capkova L, Muller P, Skladal P, Bouchal P. Pull-down Assay on Streptavidin Beads and Surface Plasmon Resonance Chips for SWATH-MS-based Interactomics. Cancer Genom Proteom. 2018;15:395-404.
57. Kang HK, Min SK, Jung SY, Jung K, Jang DH, Kim OB, et al. The potential of mouse skin-derived precursors to differentiate into mesenchymal and neural lineages and their application to osteogenic induction in vivo. Int J Mol Med. 2011;28:1001-11.
58. Shin K, Lechtenberg BC, Fujimoto LM, Yao Y, Bartra SS, Plano GV, et al. Structure of human Vitronectin C-terminal domain and interaction with Yersinia pestis outer membrane protein Ail. Sci Adv. 2019;5:eaax5068.
59. Andreu D, Albericio F, Sole NA, Munson MC, Ferrer M, Barany G. Formation of disulfide bonds in synthetic peptides and proteins. Methods Mol Biol. 1994;35:91-169.
60. Iida JBMPNSTFAW. Coordinate role for proteoglycans and integrins in cell

adhesion. 1993:127-47 .

61. Sarrazin S, Lamanna WC, Esko JD. Heparan sulfate proteoglycans. Cold Spring Harb Perspect Biol. 2011;3:a004952.
62. Loftus JC, O'Toole TE, Plow EF, Glass A, Frelinger AL, 3rd, Ginsberg MH. A beta 3 integrin mutation abolishes ligand binding and alters divalent cation-dependent conformation. Science. 1990;249:915-8.
63. Hoffman MP, Engbring JA, Nielsen PK, Vargas J, Steinberg Z, Karmand AJ, et al. Cell type-specific differences in glycosaminoglycans modulate the biological activity of a heparin-binding peptide (RKRLQVQLSIRT) from the G domain of the laminin alpha1 chain. J Biol Chem. 2001;276:22077-85.
64. San Antonio JD, Winston BM, Tuan RS. Regulation of chondrogenesis by heparan sulfate and structurally related glycosaminoglycans. Dev Biol. 1987;123:17-24.
65. Newton PT, Staines KA, Spevak L, Boskey AL, Teixeira CC, Macrae VE, et al. Chondrogenic ATDC5 cells: an optimised model for rapid and physiological matrix mineralisation. Int J Mol Med. 2012;30:1187-93.
66. Rucci N, Rufo A, Alamanou M, Capulli M, Del Fattore A, Ahrman E, et al. The glycosaminoglycan-binding domain of PRELP acts as a cell type-specific NF-kappa B inhibitor that impairs osteoclastogenesis. J Cell Biol. 2009;187:669-83.
67. Irie A, Takami M, Kubo H, Sekino-Suzuki N, Kasahara K, Sanai Y. Heparin enhances osteoclastic bone resorption by inhibiting osteoprotegerin activity. Bone. 2007;41:165-74.
68. Johnson GL, Lapadat R. Mitogen-activated protein kinase pathways mediated by

ERK, JNK, and p38 protein kinases. Science. 2002;298:1911-2.

69. Grigoriadis AE, Wang ZQ, Cecchini MG, Hofstetter W, Felix R, Fleisch HA, et al. C-Fos - a Key Regulator of Osteoclast-Macrophage Lineage Determination and Bone Remodeling. Science. 1994;266:443-8.
70. Arai F, Miyamoto T, Ohneda O, Inada T, Sudo T, Brasel K, et al. Commitment and differentiation of osteoclast precursor cells by the sequential expression of c-Fms and receptor activator of nuclear factor kappaB (RANK) receptors. J Exp Med. 1999;190:1741-54.
71. Hsu HL, Lacey DL, Dunstan CR, Solovyev I, Colombero A, Timms E, et al. Tumor necrosis factor receptor family member RANK mediates osteoclast differentiation and activation induced by osteoprotegerin ligand. P Natl Acad Sci USA. 1999;96:3540-5.
72. Aggarwal S, Singh P, Topaloglu O, Isaacs JT, Denmeade SR. A dimeric peptide that binds selectively to prostate-specific membrane antigen and inhibits its enzymatic activity. Cancer Res. 2006;66:9171-7.
73. Thamri A, Letourneau M, Djoboulian A, Chatenet D, Deziel E, Castonguay A, et al. Peptide modification results in the formation of a dimer with a 60-fold enhanced antimicrobial activity. Plos One. 2017;12(3):e0173783.
74. Gunasekera S, Muhammad T, Stromstedt AA, Rosengren KJ, Goransson U. Backbone Cyclization and Dimerization of LL-37-Derived Peptides Enhance Antimicrobial Activity and Proteolytic Stability. Front Microbiol. 2020;11:168.
75. Chen YQ, Li T, Li JG, Cheng SY, Wang JH, Verma C, et al. Stabilization of peptides against proteolysis through disulfide-bridged conjugation with synthetic

aromatics. Org Biomol Chem. 2017;15:1921-9.

76. Lee JY, Choo JE, Choi YS, Lee KY, Min DS, Pi SH, et al. Characterization of the surface immobilized synthetic heparin binding domain derived from human fibroblast growth factor-2 and its effect on osteoblast differentiation. Journal of Biomedical Materials Research Part A. 2007;83a:970-9.
77. Palchesko RN, Romeo JD, McGowan KA, Gawalt ES. Increased osteoblast adhesion on physically optimized KRSR modified calcium aluminate. Journal of Biomedical Materials Research Part A. 2012;100a:1229-38.
78. Schuler M, Hamilton DW, Kunzler TP, Sprecher CM, de Wild M, Brunette DM, et al. Comparison of the Response of Cultured Osteoblasts and Osteoblasts Outgrown From Rat Calvarial Bone Chips to Nonfouling KRSR and FHRRIKA-Peptide Modified Rough Titanium Surfaces. J Biomed Mater Res B. 2009;91b:517-27.
79. Rezania A, Healy KE. Biomimetic peptide surfaces that regulate adhesion, spreading, cytoskeletal organization, and mineralization of the matrix deposited by osteoblast-like cells. Biotechnol Progr. 1999;15:19-32.
80. Hozumi K, Kobayashi K, Katagiri F, Kikkawa Y, Kadoya Y, Nomizu M. Syndecan- and integrin-binding peptides synergistically accelerate cell adhesion. FEBS Lett. 2010;584:3381-5.
81. Lees RL, Heersche JNM. Macrophage colony stimulating factor increases bone resorption in dispersed osteoclast cultures by increasing osteoclast size. J Bone Miner Res. 1999;14:937-45.
82. Hodge JM, Collier FM, Pavlos NJ, Kirkland MA, Nicholson GC. M-CSF

Potently Augments RANKL-Induced Resorption Activation in Mature Human Osteoclasts. Plos One. 2011;6:e21462.

83. Lee PS, Wang Y, Dominguez MG, Yeung YG, Murphy MA, Bowtell DD, et al. The Cbl protooncoprotein stimulates CSF-1 receptor multiubiquitination and endocytosis, and attenuates macrophage proliferation. EMBO J. 1999;18:3616-28.
84. Ji JD, Park-Min KH, Shen ZX, Fajardo RJ, Goldring SR, McHugh KP, et al. Inhibition of RANK Expression and Osteoclastogenesis by TLRs and IFN-gamma in Human Osteoclast Precursors. Journal of Immunology. 2009;183:7223-33.
85. Takami M, Kim N, Rho J, Choi Y. Stimulation by toll-like receptors inhibits osteoclast differentiation. Journal of Immunology. 2002;169:1516-23.
86. Chang EJ, Kim HJ, Ha J, Kim HJ, Ryu J, Park KH, et al. Hyaluronan inhibits osteoclast differentiation via toll-like receptor 4. J Cell Sci. 2007;120:166-76.
87. Patel J, Kothari R, Tunga R, Ritter N, Tunga B. Stability considerations for biopharmaceuticals: overview of protein and peptide degradation pathways. BioProcess International. 2011;9:2-11.
88. “Peptide Storage and Handling Guidelines”, GeneScripts homepage, updated assessed July 5, 2020, https://www.genscript.com/peptide_storage_and_handling.html/.
89. Calce E, Vitale RM, Scaloni A, Amodeo P, De Luca S. Air oxidation method employed for the disulfide bond formation of natural and synthetic peptides. Amino Acids. 2015;47:1507-15.

# 국문 초록

# 인간 비트로넥틴 유래 이량체 펩티드 발굴 및 파골세포 분화 조절에 미치는 효과

정 성 윤

종양 및 발달생물학 전공

서울대학교 대학원 치의과학과

(지도교수: 민 병 무, D.D.S., M.S., Ph.D.)

세포외기질단백질은 세포 부착, 이동, 분화, 증식 등 세포거동을 조절하므로 세포외기질단백질의 활성부위를 규명하여 생체활성 펩티드를 발굴하여 재생의학 및 조직공학에 이용하려는 연구가 활발히 이루어져 왔다. 펩티드는 합성의 용이성, 낮은 면역원성, 구조 및 기능적 유연성 등 많은 장점을 가지고 있다. 본 연구는 사람 비트로넥틴에서 세포활성을 갖는 생체활성 펩티드를 발굴하고, 발굴한 펩티드가 파골세포 분화 및 그의 분자기작에 미치는 영향에 관하여 연구하였다. 즉, 뼈 기질단백질인 사람 비트로넥틴의 homopexin

유사 도메인 1 에서 골모세포유사세포의 세포부착을 촉진시키는 12개 아마노산 잔기로 이루어진 펩티드(VnP-8)를 동정하였다. VnP-8 펩티드는 자연적 산화반응에 의해 C-말단에서 isoleucine 잔기가 제거되고 이황화결합에 의해 결합됨으로써 이량체인 VnP-8-DN1 dimer 펩티드를 형성하였다. VnP-8-DN1 dimer는 VnP-8보다 골모세포의 세포 부착과 퍼짐을 유의하게 촉진시켰으며, 헤파린 부착능을 보였고, 파골세포전구세포에서 파골세포로의 분화를 유의하게 억제시켰다. 펩티드를 배지에 첨가하였을 때에도 VnP-8-DN1 dimer는 파골세포의 초기 분화단계에 작용하여 파골세포 분화를 억제시켰다. 또한 VnP-8-DN1 dimer는 파골세포 분화에 중요한 M-CSF 또는 RANKL에 의해 유도되는 MAPKs 신호전달계를 억제하였으며 파골세포전구세포의 생존을 증가시키고, M-CSF의 세포표면수용체인 c-Fms 발현을 감소시켰다. 이는 VnP-8-DN1 dimer가 M-CSF 신호전달경로에 영향을 미친다는 것을 의미한다. 특히, VnP-8-DN1 dimer는 c-Fms와 상호작용하여 c-Fms의 세포 내 수준을 감소시켰고 RANK의 발현을 감소시켜 파골세포 분화를 억제시킴을 규명하였다. 본 연구결과를 종합할 때, VnP-8-DN1 dimer는 골모세포유사세포의 세포 부착을 촉진하고 파골세포전구세포에서 파골세포로의 분화를 조절함으로써 골질환 치료 및 골조직 재생에 유용한 치료제로 사용될 수 있을 것으로 생각된다.

---

**주요어:** I D A A F T R I N C Q G 모티프, 11-mer 이량체 펩티드, 세포거동,

파골세포 분화, c-Fms, 골 재생

**학 번:** 2016-36909